Joint stochastic optimization of open pit mine production scheduling, ramp design and cut-off grades for multiple elements under geological uncertainty

Jacob Cutler

A thesis submitted to McGill university in partial fulfillment of the requirements of the degree of

Master of Science

Department of Mining and Materials Engineering

McGill University, Montreal, Quebec, Canada

August 2024

Acknowledgements

I would like to express my deepest gratitude to my supervisor, Prof. Roussos Dimitrakopoulos, for giving me the opportunity to be part of the COSMO laboratory. His support, teaching, and mentorship through my master's degree have been pivotal in shaping my research journey.

My heartfelt thanks extend to the entire COSMO lab team. Cristina, your encouragement and support made even the most daunting of tasks seem achievable. João, your wisdom and patience not only made me a better researcher but also brought daily joy and laughter to our office. Liam, your kindness and openness created a welcoming atmosphere that made the lab feel like home. Laura, your guidance and support kept me focused and on the right path, and your exceptional party-planning skills added a spark of joy to our team. Zach and Yassine, your generosity in sharing your expertise and advice aided my growth tremendously. I am also deeply grateful to Will, Victor, Fred, Athenaïs, and Lingqing for their shared knowledge and support. A special thanks to Kelly and Caroline for their exceptional administrative support, which ensured that everything ran smoothly in the lab.

I extend my appreciation to all COSMO sponsors for their invaluable financial and technical support, notably the Natural Sciences and Engineering Research Council (NSERC) of Canada, CRD Grant CRDPJ 500414-16, and the COSMO Mining Industry Consortium (AngloGold Ashanti, BHP, De Beers, Anglo American, IAMGOLD, Kinross, Newmont, and Vale), along with NSERC Discovery Grant 239019.

To my dear friends in Montreal, Caio, Ali, Elif, Rhys, Diego, Loc, Zach, and Rohan, your kindness and the memories we've created together are treasured. I will look back at our post-gym dinner parties fondly for many years to come. Though life has taken us on different paths and to different cities, I hold onto the hope that our paths will cross again.

Above all, my deepest appreciation goes to my parents, Rob and Ora-Lee, whose belief in me made all this possible. To my brothers, thank you for your unwavering support and invaluable guidance. Your constant encouragement and belief in my abilities have been a source of strength throughout my academic journey.

Contribution of Authors

For all work presented herein, the primary author is the author of this thesis. All work was completed under the supervision and advice of Prof. Roussos Dimitrakopoulos, who is also a co-author of the two papers.

Chapter 2 - Cutler, J., & Dimitrakopoulos, R. (2024). Joint stochastic optimisation of open pit mine production scheduling with ramp design. International Journal of Mining, Reclamation and Environment, 38(6), 480–495. https://doi.org/10.1080/17480930.2024.2335709

Chapter 3 – Cutler J., & Dimitrakopoulos, R. (2024). Optimizing multi-element cut-off grades for a strategic production plan under geological uncertainty. International Journal of Mining, Reclamation and Environment, Submitted, 2024

Abstract

Strategic planning involves determination of the production schedule, destination policy, and down-stream decisions. Traditionally, these components are optimized sequentially, beginning with the destination policy, formulated as a cut-off grade optimized through Lane's method. Next the production schedule is optimized, defining when and where to extract material, however equipment access is largely ignored at this stage. Lastly, down-stream decisions are optimized, defining how material is distributed and treated. Importantly, all these components depend upon each other, meaning sequential optimization results in a local optimum, rather than a globally optimal strategic plan. Additionally, traditional approaches to strategic planning are deterministic, ignoring the uncertainty inherent in mine planning. Significant improvements over the traditional strategic planning practices have been developed, providing methods that consider multiple sources uncertainty, such as geological, equipment performance, and market uncertainty, and simultaneously optimize production schedules, destination policies, and down-stream decisions under a single mathematical formulation. However, these developments do not explicitly consider equipment access constraints when optimizing the production schedule, and do not provide cut-off grades for multiple elements. Recent studies have developed methods for optimizing production schedules and ramp designs, but do not consider uncertainty and explicit equipment access to mining blocks. Additionally, research on optimizing cut-off grades has largely focused on deterministic methods for single elements with a stockpile and processor. Optimizing multi-element cut-off grades with multiple destinations under geological uncertainty has not received treatment in literature. In this thesis, two methods are proposed for addressing (1) the joint stochastic optimization of long-term open pit production schedules with ramp design, while ensuring feasible equipment access to mining blocks, and (2) the determination of optimal long-term multi-element cut-off grade policies under geological uncertainty from an optimal production plan is presented.

The first chapter in this thesis presents a literature review on deterministic and stochastic mine planning developments, and geostatistical simulation methods. The concept of a mining complex as it relates to the traditional framework, geological uncertainty, and the state-of-the-art simultaneous stochastic optimization is introduced. Next, deterministic optimization methods for production schedules, cut-off grades, and ramp design are presented. A review of geostatistical

simulation methods follows, covering gaussian, multi-point, and high-order methods follows. Lastly, state-of-the-art literature on simultaneous stochastic optimization of mining complexes is reviewed.

The second chapter presents a new two-stage stochastic integer programming formulation for jointly optimizing long-term open pit mine production schedules and ramp design while ensuring feasible equipment access to mined blocks under geological uncertainty. The objective function aims to maximize value while considering the cost required for placing and removing ramps, while managing risk. A case study is presented at a gold mine, demonstrating the methods ability to generate operationally feasible schedules and ramp designs that manage risk of deviating from production targets.

The third chapter in this thesis presents a reinforcement learning framework for optimizing multi-element cut-off grades under geological uncertainty for optimal production schedules. The method aims to produce long-term multi-element cut-off grade policies minimizing deviations from optimal production forecasts. Two possible multi-element cut-off grades are presented: Orthogonal, and Diagonal, and tested at a gold-copper mining complex. Both multi-element cut-off grades are shown to meet production forecasts, with the Diagonal cut-off grade performing slightly better.

Future research in theses areas may explore integrating the joint optimization of long-term open pit mine production schedules with ramp design into the larger simultaneous stochastic optimization of mining complexes framework and investigate alternative multi-element cut-off grades.

Resume

La planification stratégique implique la détermination du calendrier de production, de la politique de destination et des décisions en aval. Traditionnellement, ces composantes sont optimisées de manière séquentielle, en commençant par la politique de destination, formulée sous forme de teneur de coupure optimisée par la méthode de Lane. Ensuite, le calendrier de production est optimisé, définissant quand et où extraire le matériau, cependant, l'accès des équipements est largement ignoré à ce stade. Enfin, les décisions en aval sont optimisées, définissant comment le matériau est distribué et traité. Il est important de noter que toutes ces composantes dépendent les unes des autres, ce qui signifie qu'une optimisation séquentielle conduit à un optimum local, plutôt qu'à un plan stratégique globalement optimal. De plus, les approches traditionnelles de la planification stratégique sont déterministes, ignorant l'incertitude inhérente à la planification minière. Des améliorations significatives par rapport aux pratiques traditionnelles de planification stratégique ont été développées, proposant des méthodes qui prennent en compte plusieurs sources d'incertitude, telles que les incertitudes géologiques, de performance des équipements, et du marché, et optimisent simultanément les calendriers de production, les politiques de destination et les décisions en aval sous une seule formulation mathématique. Cependant, ces développements ne considèrent pas explicitement les contraintes d'accès des équipements lors de l'optimisation du calendrier de production, et ne fournissent pas de teneurs de coupure pour plusieurs éléments. Des études récentes ont développé des méthodes pour optimiser les calendriers de production et la conception des rampes, mais ne prennent pas en compte l'incertitude ni l'accès explicite des équipements aux blocs miniers. De plus, la recherche sur l'optimisation des teneurs de coupure s'est largement concentrée sur des méthodes déterministes pour des éléments uniques avec un stock et un processeur. L'optimisation des teneurs de coupure multi-éléments avec plusieurs destinations sous incertitude n'a pas été traitée dans la littérature. Dans cette thèse, deux méthodes sont proposées pour aborder les deux problèmes mentionnés précédemment. Premièrement, une méthode d'optimisation conjointe des calendriers de production à long terme des mines à ciel ouvert et de la conception des rampes, tout en garantissant un accès viable des équipements aux blocs minés, est présentée. Deuxièmement, une méthode pour déterminer les teneurs de coupure multi-éléments optimales sous incertitude à partir d'un plan de production optimal est présentée.

Le premier chapitre de cette thèse présente une revue de la littérature sur les développements en planification minière déterministe et stochastique, ainsi que sur les méthodes de simulation géostatistique. Le concept d'un complexe minier en relation avec le cadre traditionnel, l'incertitude géologique et l'optimisation stochastique simultanée à la pointe de la technologie est introduit. Ensuite, les méthodes d'optimisation déterministes pour les calendriers de production, les teneurs de coupure et la conception des rampes sont présentées. Une revue des méthodes de simulation géostatistique suit, couvrant les méthodes gaussiennes, multi-points et d'ordre supérieur. Enfin, la littérature de pointe sur l'optimisation stochastique simultanée des complexes miniers est examinée.

Le deuxième chapitre présente une nouvelle formulation de programmation stochastique en deux étapes pour l'optimisation conjointe du calendrier de production à long terme des mines à ciel ouvert et de la conception des rampes, tout en garantissant un accès viable des équipements aux blocs minés sous incertitude géologique. La fonction objective vise à maximiser la valeur tout en prenant en compte le coût requis pour placer et retirer les rampes, en gérant le risque. Une étude de cas est présentée dans une mine d'or, démontrant la capacité des méthodes à générer des calendriers et des conceptions de rampes opérationnellement faisables qui gèrent le risque de déviation, par rapport aux objectifs de production.

Le troisième chapitre de cette thèse présente un cadre d'apprentissage par renforcement pour l'optimisation des teneurs de coupure multi-éléments sous incertitude géologique pour des calendriers de production optimaux. La méthode vise à produire des politiques de teneur de coupure multi-éléments à long terme minimisant les écarts par rapport aux prévisions de production optimales. Deux teneurs de coupure multi-éléments possibles sont présentées : Orthogonale et Diagonale, et testées dans un complexe minier d'or et de cuivre. Les deux teneurs de coupure multi-éléments montrent qu'elles respectent les prévisions de production, la teneur de coupure Diagonale offrant des performances légèrement meilleures.

Les recherches futures dans ces domaines pourraient (1) explorer l'intégration de l'optimisation conjointe des calendriers de production à long terme des mines à ciel ouvert avec la conception des rampes dans le cadre plus large de l'optimisation stochastique simultanée des complexes miniers et (2) enquêter sur les alternatives des teneurs de coupure multi-éléments.

Table of Contents

List of Figures

List of Tables

Chapter 1. Introduction and Literature Review

A mining complex is an interconnected system, in which raw material flows from its in-situ source, through transformative intermediary value adding destinations, and eventually out to the market (Pimentel et al., 2010; Goodfellow and Dimitrakopoulos, 2016; Montiel et al., 2016). Traditionally, such a system is optimized sequentially, where individual components are optimized in isolation, relying on estimated inputs. First, a cut-off grade policy is optimized using Lane's method, which relies on the global distribution of material (Lane, 1988). Next, the so-called ultimate pit limit is determined using Lerch Grossman, relying on block values determined from estimated grades (Lerchs and Grossman, 1965). Next pushbacks may be determined from a nested-pits procedure where the value of metal is varied, after which a schedule may finally be determined. However, at all steps in the traditional process, uncertainty is ignored, and synergies that may exist between the various components of the mining complex are unable to be captured (Whittle, 2007).

Of the many sources of uncertainty ignored in the traditional framework, geological uncertainty is the most impactful. Baker and Giacomo (2001) published a study showing that geological uncertainty is the main factor for not meeting production targets. Vallee (2000) further demonstrates the impact of geological uncertainty on mining operations, showing significant deviations from forecasted ore reserves, and realized production within the first year. Dimitrakopoulos et al. (2002) show that forecasts based upon deterministic inputs differ significantly from forecasts obtained from simulated inputs, and that including uncertainty enables risk to be quantified and incorporated into the planning process. For these reasons stochastic mine planning has seen significant development, as it enables quantification of risk at every component in the value chain and considers uncertainty in every decision.

The simultaneous stochastic optimization framework optimizes all components of a mining complex simultaneously, considering all sources of uncertainty. Under this framework, it is useful to model a mining complex as a graph, where nodes represent locations that transform material, and edges represent valid material flows. The transformation applied to material at each node is often referred to as a transfer function and need not be linear. The simultaneous optimization of all components enables exploitation of advantageous relationships between components and management of deleterious relationships (Goodfellow and Dimitrakopoulos, 2016; Montiel et al., 2016). Traditional, sequential frameworks fail in this regard as each component is optimized individually of all other components. Mining operations are large, interconnected systems, which may consist of multiple mines, stockpiles, waste facilities, transportation systems, etc. In the simultaneous stochastic optimization framework, material from multiple mines may be blended to produce better feed to downstream nodes. However, in the traditional sequential framework the blending opportunity can not be fully captured as each component is optimized individually. Hoerger et al. (1999) presents one of the first applications of simultaneous optimization of a large mining complex at Newmont's Nevada operations, finding increased value because of previously uncaptured synergies. Since then, Whittle has incorporated a form of global optimization into their software, and has become the industry standard for long term planning (Whittle, 2018). Goodfellow and Dimitrakopoulos (2016) present the first simultaneous stochastic optimization framework for entire mining complexes (in-situ source to final customer), capturing synergies and managing risk.

The remainder of this chapter will discuss deterministic mine planning literature, geostatistical simulation methods and simultaneous stochastic optimization.

1.1 Deterministic Optimization

The conventional mine planning framework considers all input parameters to be known with certainty. Typically, the input parameters consist of an estimated block model, operating costs, and metal price. The operating costs, and metal prices may be forecasted to change over the life of mine, but are commonly fixed and, again, assumed to be known with certainty.

The first step of the conventional mine planning framework begins with optimization of the cut-off grade policy through Lane's method (Lane, 1988). Lane's method considers a mining operation to be limited by one of, or a combination of the mine, mill, or market. If the mining operation is limited by one of those components individually, the optimal cut-off grade is the *limiting cut-off grade* for the limiting component. However, if the mining operation is limited by more than one component, the optimal cut-off grade is a *balancing cut-off grade* of the limiting components. In total, there are 6 possible cut-off grades that may provide the optimal value (3 limiting and 3 balancing). Lane's method provides optimal cut-off grade for each period over the life of mine, considering the global distribution of material, however, the global distribution of material differs significantly from the distribution of material available in each year once a production schedule has been defined.

In its original form, Lane's method is equipped to deal with stockpiles, and multi element mines with different market conditions/requirements. However, this approach to stockpile management is not necessarily optimal, as any material with a grade above the lowest cut-off grade over the life-of mine and below the current cut-off grade is stockpiled. Additionally, convergence of Lane's method becomes problematic in for multiple elements. Asad (2005) presents an implementation of Lane's method for two elements with stockpiling, addressing the issue of convergence with a grid search technique. However, any material with a grade above the marginal cut-off grade and below Lane's cut-off grade is stockpiled, and all stockpiled material is processed only after mining concludes. Ganguli (2011) presents a mixed integer linear program (MILP) for multi-element cut-off grade optimization, considering operational constraints and sequencing, however, the method does not directly optimize cut-off grades, rather material destinations are optimized. Additionally, none of these methods are suitable for optimizing multi-element cut-off grades when more than a stockpile and processor destination are available for ore.

Once the cut-off grade policy is determined, a series of nested pits are computed by varying the commodity price. Each nested pit corresponds to the ultimate pit limit for the associated commodity price, and is entirely contained within nested pits associated with higher prices (Lerchs and Grossman, 1965; Seymour, 1995). Note, here, the ultimate pit limit corresponds to the pit extents that maximize the undiscounted cashflow, rather than the extents of the pit that contains the schedule which maximizes NPV. This property makes nested pits useful to guide the direction of mining and design pushbacks. The ultimate pit problem was first formulated as graph problem in (Lerchs and Grossman, 1965). More recent methods for solving the ultimate pit frame the problem as a maximum flow problem, where ore blocks are connected to the source with a capacity equal to the value of the block, waste blocks are connected to the sink with a capacity equal to the absolute block value, and internal arcs of infinite capacity connect predecessors and successors. After solving the maximum flow, any ore block with incoming flow from the source less than its block value is in the ultimate pit. Presently the fastest algorithm for solving such a problem is the pseudo-flow algorithm presented in (Hochbaum, 2008). The nested pits can then be grouped into pushbacks, which are used to guide the direction of mining, and grouped to maximize NPV while satisfying operational constraints such as mining width. Once pushbacks are defined the production schedule can be determined, constrained to the sequence of mining defined by the pushbacks.

In the traditional approach described above, each component is optimized individually, first the cut-off grade is optimized without a production schedule, followed by the pushbacks and extraction sequence. Such a procedure leads to local optimal solutions, rather than a global optimal. Hoerger et al. (1999) present a linear program that optimizes multiple mines, and material flow from the mines to shared resources in the Carlin trend. Though the model had several limitations: (1) blocks were grouped into push backs, (2) non-linear transformations such as blending and stockpiling are not included in, and (3) uncertainty is ignored. However, optimizing multiple components in a single mathematical modeled captured more value than the traditional sequential framework.

Whittle (2007) also recognized the shortcomings of the sequential optimization approach and incorporated more components of mine planning into a single mathematical framework. The prober optimizer incorporated in the whittle software randomly samples feasible solutions and locally optimizes each sample. This process does not guarantee a global optimal solution; however, sufficient samples should provide confidence in the quality of the solution. Additionally, many steps are required to reduce the problem to a tractable size, such as aggregation of mining blocks into panels and parcels of material. None the less, the whittle software has become the industry standard, and their approach has provided significant value (Whittle, 2018).

Similarly, the BHP mine planning optimisation group also recognized the value of simultaneous optimization. Stone et al. (2004) presents the BLASOR optimizer, and its application to the Yandi mining complex. The Yandi mining complex consisted of 11 open pits, to be scheduled over 20 periods, with strict product requirements on the marketable ore. Material is not classified as waste or ore a priori, the classification/destination of material is optimized by BLASOR. To reduce the optimization problem to a tractable size, BLASOR relies on an aggregation technique, where groups of blocks with similar properties are clustered together, reducing the number of decision variables required for optimizing the extraction sequence. Extraction scheduling is performed of the aggregated groups of blocks, which is then used for phase design, and lastly, panel sequencing.

However, notably, human input is required for the phase design to ensure mineability and preventing “rat-holing”.

Optimizing a production schedule, while ensuring mineability is complex, as equipment access must be ensured for every block in the period in which it is mined. As a result, most approaches do not provide an explicit guarantee, instead, softer constraints, such as mining width and sink rate are used promote more mineable schedules. However, these do not explicitly guarantee mineability, as space for ramps is not considered, and the mining width constraint is insufficient to guarantee that a suitable surface for a road exists. Yarmuch et al. (2021) presents a binary integer program (BIP) for optimizing mineable pushback designs considering access, however, the method optimizes cashflow, rather than NPV, and requires tuning of hyper-parameters to ensure mineable shapes.

The simultaneous optimization approaches provide significant value compared to the traditional sequential optimization framework. However, the presented methods discussed above all share several common limitations: (1) they do not consider uncertainty, relying solely on deterministic inputs, and (2) simplification procedures are used to reduce the size of the problem, however, simplification techniques artificially reduce selectivity, reducing NPV.

1.2 Modeling Supply Uncertainty and Spatial Variability

Supply uncertainty presents a significant challenge for mining operations and is the greatest contributor to deviations from forecasted performance (Vallee, 2000; Baker and Giacomo, 2001). Quantifying the uncertainty and variability of the in-situ grades is critical to mine planning, enabling risk aware forecasts, and better decision making (Ravenscroft, 1992; Dowd, 1994; Dowd, 1997; Dimitrakopoulos et al., 2002).

The goal of spatial modeling is to determine the attribute value z at all locations u in the domain D of interest. Estimation methods, provide the best local estimate in the least squares sense, estimating the value of z at location u, $z^*(u)$ as the value that minimizes $Var\{Z^*(u) - Z(u)\}$. However, maps of local best estimates smooth out local variability and are not best in a global sense. Estimation methods, by construction, tend to overestimate low values and under estimate high values (David, 1977; Journel and Huijbregts, 1978; David, 1988; Isaaks and Srivastava, 1989;

Goovaerts, 1997; Rossi and Deutsch, 2014). The smoothing effect of estimation methods has serious implications for mine planning, as high grade values, and their connectivity drive value (de Carvalho and Dimitrakopoulos, 2019). Additionally, mining operations are complex systems, where material undergoes numerous non-linear transformations on its journey from it in-situ source to its final destination. The non-linearity of the transformations is critically important for mine planning because $E[f(x)] \neq f(E[x])$ if $f(\cdot)$ is a non-linear function, meaning that forecasts produced from estimated models may be misleading, as shown in Dimitrakopoulos et al. (2002). Conversely, stochastic methods provide equiprobable realizations that reproduce the desired statistics of the conditioning data, such as the mean, variance, variogram, etc….

Geostatistical simulations employ the random function (RF) model, where the values of z at unknown locations u are regarded as spatially corelated random variables. The random variable (RV) at location u, $Z(u)$ is fully characterized by its conditional cumulative probability function (cdf) $F(u; z) = Prob\,\{Z(u) \leq z\}$ (Goovaerts, 1997). Given conditioning data $\Lambda = \{u_\alpha, \alpha = 1, \dots, n\}$, simulated realizations which reproduce the desired statistic can be generated by sampling the N-variate ccdf modeling the joint uncertainty at N locations $F\big(u_i', \dots, u_N'; z_1, \dots, z_N \big| (\Lambda)\big) = Prob\{Z(u_i') \leq z_1, \dots, Z(u_N') \leq z_N | (\Lambda)\}$. The commonly employed sequential simulation paradigm recursively employs Baye's axiom to decompose the N-variate ccdf of the RV $Z(u)$ into the product of N one-point ccdfs $F\big(u_i', \dots, u_N'; z_1, \dots, z_N \big| (\mathrm{n})\big) = f(u_1,\, z_1 | (n)) \cdot f\big(u_2; z_2 \big| (n+1)\big) \cdot \dots \cdot f\big(u_N; z_N \big| (n+N-1)\big) = \prod_{i=1}^{N} f(u_i; z_i | (n+i-1))$, enabling each location $u_i, i = 1, \dots, N$ to be simulated sequentially.

Modelling of the subsurface is a challenging task as the available data is usually sparse, and the properties of interest may exhibit complex spatial patterns. This chapter will first discuss Gaussian simulation methods, which reproduce second-order spatial statistics. Next multi-point simulation methods will be discussed, which can reproduce complex structures, but rely heavily on training images. Lastly, high-order simulation methods will be presented, which share many of the desirable properties of multi-point methods, without relying as strongly on training images.

1.2.1 Sequential Gaussian Simulation

Sequential Gaussian simulation (SGS) relies on the multi-Gaussian assumption, under which, the conditional distribution of any RV $Z(\boldsymbol{u})$, given conditioning data (n) of another subset is also

Multi-gaussian (Abramowitz and Stegun, 1964). Under this assumption, the mean and variance of any gaussian ccdf are identical to the simple kriging mean and variance (Journel and Huijbregts, 1978), allowing the ccdf of each node to be constructed from simple kriging. The general steps of sequential gaussian simulation are as follows.

1. Transform the conditioning data into Gaussian space.
2. Define a random path visiting each node to be simulated exactly once.
3. Select the next empty node in the path.
4. Compute the kriging mean and variance for the selected node.
5. Construct and sample the Gaussian ccdf with mean and variance defined above.
6. Add the simulated value to the conditioning set.
7. Repeat from 3 for all nodes in path.
8. Back transform the simulated values into data space.
9. Validate the results (mean, variance, histogram, variogram, etc…)

Two notable limitations of SGS are: (1) the gaussian distribution maximizes entropy, maximizing spatial disorder beyond the covariance model (Journel and Deutsch, 1993) , negatively effecting connectivity of extreme values , and (2) identification of the conditioning data for calculation of the mean and variance is computationally expensive and SGS requires a significant amount of redundant searching. The following methods presented below address these concerns to some extent by changing the structure of the random path and reducing the number of redundant spatial searches for conditioning data.

1.2.2 LU Simulation

Davis (1987) introduces conditional simulation through lower-upper (LU) decomposition of the covariance matrix. The simulated map of values is defined as $z = Lw$, where L is the lower triangular decomposition of the covariance matrix C, and w is a vector of independent $N(0,1)$ random values. Similarly, conditional LU simulation is defined as $z = L_{gd}L_{dd}^{-1}z' + L_{gg}w$, where z' is the conditioning data, L_{gd} is grid-data portion of the decomposed covariance matrix, L_{dd} is the data-data covariance portion, and L_{gg} is the grid-grid covariance portion. Inversion of L_{dd} is computationally expensive, unstable, and can be avoided by solving $L_{dd}^{T}x^{T} = L_{gd}^{T}$ (transposed as most linear algebra libraries provide solved of the form Ax=b, rather than xA=b), which, is very efficient since L_{dd} is triangular. After solving for x, the resulting simulation algorithm is $z = xz' + L_{gg}w$. Though this method may eliminate redundant special searching of conditioning data, it quickly becomes intractable as the size of the simulation domain increases. The required covariance matrix is a square matrix with side length of $(n + N)$, where n is the number of conditioning data, and N is the number of points to simulate. As a result, the memory requirements are $(n + N)^2$, and the time complexity is $O((n + N)^3)$.

1.2.3 Generalized Sequential Gaussian Simulation

Dimitrakopoulos and Luo (2004) provides a generalization of SGS and LU simulation, where groups of nearby nodes are simulated simultaneously. Simulating nearby nodes simultaneously reduces redundant spatial searching as nearby nodes are likely to share conditioning data, and only one spatial search is required for each group. With screen effect approximation, where only $v_{\max}$ conditioning data may be used, the running time of SGS is $O(Nv_{max}^3)$, LU is $O(v_{max} + N)^3)$, and GSGS is $O(\frac{N}{v}(v_{max} + v)^3)$, where v is the group size. From a purely computational perspective GSGS achieves its best performance when $v = 0.8v_{max}$, however, the quality of the simulation should also be considered. GSGS is sensitive to the group size and neighborhood size, and a small neighborhood size can lead to artifacts.

1.2.4 Direct Block Simulation

Godoy (2003) presents a direct block simulation algorithm (DBSIM), substantially reducing memory requirements and speeding up simulations. In this method, the internal points of a block are simulated using the group decomposition approach of GSGS, then (1) the internal points are back transformed from normal space to data space and averaged into a block value which can be exported to a file and discarded, and (2) the points are averaged into a block value in normal space and stored in the conditioning set. The construction of the covariance matrix involves determining point-block covariance, and the block-block covariance values. The point-block covariance can be computed as the volumetric average of the point-point covariance between the point u_0 and all internal points of the volume as follows.

$$C(u_0, v) = \frac{1}{|V|}\int_v C(u_0.u)du \approx \frac{1}{|V|}\sum_v C(u_0, u_v) \tag{1}$$

Similarly, the block-block covariance can be computed as:

$$C(v_a, v_b) = \frac{1}{|V_a|\,|V_b|} \int_{v_a} \int_{v_b} C(u_a.u_b) du_a du_b \approx \frac{1}{|V_a|\,|V_b|} \sum_{v_a} \sum_{v_b} C(u_a, u_b) \tag{2}$$

Averaging internal nodes into a block values, and discarding the simulation points significantly reduces memory requirements. Compared to SGS, if the simulation grid is intended to be re-blocked with $[N_x, N_y, N_z]$ internal nodes in each block, then DBSIM would require $\frac{1}{N_x * N_y * N_z}$ as much memory. Additionally, DBSIM realizations exhibit better connectivity than SGS realizations, which may be attributed to the structure of the path.

1.2.5 Simulation of Multiple Attributes

The methods presented above simulate single attributes, however, it is common for orebody models to be contain multiple attributes. The above methods can be adapted to simulate multiple attributes, but require fitting many cross-covariance models, and expand the covariance matrix considerably. Another approach is to first decorrelate the attributes, simulate each decorrelated attribute independently, then back transform the decorrelated realizations into dataspace. Such an approach eliminates the need to model cross-variograms and does not require larger covariance matrices.

Desbarats and Dimitrakopoulos (2000) simulate multiple attributes by decorrelating with minimum/maximum autocorrelation factors (MAF). The general steps to simulating with MAF are as follows.

1. Transform data into normal space $Z(u) = \{Z^1(u), Z^2(u), \dots, Z^k(u)\} \rightarrow Y(u) = \{Y^1(u), Y^2(u), \dots, Y^k(u)\}$
2. Compute the linear model of coregionalization $\Gamma_Y(h) = \sum_s B_s \gamma_s(h)$
$$B = \lim_{||\mathrm{h}|| \to \infty} \Gamma_Y(h)$$
3. Transform the normal scores into independent MAF facts by $F_{MAF}(u) = MY(u)$
    a. Computing M
        i. Compute Spectral decomposition $B = Q^T \Lambda Q$
        ii. Rotate normal score variables to PCA factors $Y_{PCA}(u) = \Lambda^{-\frac{1}{2}} QZ(u)$
        iii. LMC of Y_{PCA}: $\Gamma_{Y_{PCA}}(h) = ABA^T \gamma_1(h) + AB_0 A^T \big(\gamma_0(h) - \gamma_1(h)\big) A^T$
$$ABA^T = I$$

$$AB_0A^T = V$$

iv. Compute spectral decomposition $V = Q_1^T \Lambda_1 Q_1$

v. Rotate PCA factors using eigenvectors of V

$$F_{MAF}(u) = Q_1 Y_{PCA}(u) = Q_1 AZ(u) = Q\Lambda^{-1\backslash 2} QZ(u) = MZ(u)$$

4. Simulate MAF factors independently
5. Back transform to normal score space $Y(u) = A^{-1} Q_1^T F_{MAF}(u)$
6. Back transform to data space $Y(u) = \{Y^1(u), Y^2(u), \ldots, Y^k(u)\} \rightarrow Z(u) = \{Z^1(u), Z^2(u), \ldots, Z^k(u)\}$

Using this method (Desbarats and Dimitrakopoulos, 2000) simulated multiple pore-sizes, reproducing the cross-relations between different pore sizes. Boucher and Dimitrakopoulos (2007), and Boucher and Dimitrakopoulos (2009) present direct block simulation with MAF (DBMAFSIM), which follows the same algorithm as DBSIM, with the addition of a back rotation of the internal nodes transforming the values into normal space, before the normal to data space transform is performed.

1.2.6 Multi-point Simulation

The Gaussian simulation methods presented above reproduce second-order statistics, which are suitable for Gaussian random functions. However, geological phenomena are non-Gaussian, non-linear, complex structures that cannot be faithfully reproduced with gaussian methods (Guardiano and Srivastava, 1993; Strebelle, 2002; Journel, 2003). Multi-point simulation methods infer higher-order statistics from a training image (TI), allowing reproduction of complex, non-Gaussian, non-linear phenomena. The training image serves as a database of spatial patterns, allowing computation of the ccdf conditioned to the available data at each simulation node.

Guardiano and Srivastava (1993) propose the ENESIM algorithm, which computes the ccdf at each simulation node by scanning the TI for replicates of the data configuration around the simulation node and storing the frequency of central node values. A value is then sampled from the histogram defined by the central node frequencies and added to the conditioning set. Though capable of reproducing complex non-Gaussian phenomena, ENESIM is computationally expensive as simulation of each node requires a full scan of the TI, making it unsuitable for large simulations with large training images. Strebelle (2002) proposes SNESIM, which improves upon

ENESIM by eliminating the need to scan the training image for each node. SNESIM introduces a tree data structure which stores central node frequencies for all observed data configurations in the training image, allowing the construction of the ccdf from a tree lookup. The tree can be constructed from a single scan of the TI, drastically reducing the computations requirements compared to ENESIM. However, these methods are limited in that they are only suitable for simulating categorical attributes.

Zhang et al. (2006) overcomes this limitation with FILTERSIM, a multiple-point simulation method suitable for continuous attributes. FILTERSIM first scans the TI, classifying all observed patterns with a filter score, which is later used to group patterns into a predefined number of bins. A representative member (prototype) for each bin is computed as the average of all patterns contained within. At each step of the simulation, a pattern sampled from the bin with the prototype that best matches the data event is pasted onto the simulation grid. An inner patch of the pasted pattern may be frozen to speed up the simulation procedure but may lead to discontinuities. Wu et al. (2008) improve upon computational aspects of FILTERSIM with a score-based distance function and dual template, enabling fast simulation of large 3D models with continuous and categorical attributes.

Mariethoz et al. (2010) proposes direct sampling for multiple-point simulation, where at each simulation node the TI is randomly scanned for a matching pattern. The TI is scanned in a random order and the distance from each observed pattern and the data event computed, and best is stored. If the observed pattern has a distance less than a predefined threshold, or the number of search iterations is reached, the best matching is pasted into the simulation grid. Mariethoz et al. (2010) also proposes syn-processing to improve pattern reproduction. Syn-processing functions by postponing the simulation of a node if the best matching pattern does not satisfy the threshold, and recursively deleting and re-simulating neighboring nodes until the threshold can be satisfied.

Straubhaar et al. (2011) propose IMPALA, an efficient and parallelizable multi-point simulation algorithm. Rather than standard tree data structures used in most multi-point methods, IMPALA uses a list to store patterns, reducing ram requirements, and facilitating easy parallelization for computation of the ccdf. The list stores tuples of (d, c), where d is the data event, and c is a vector and c_i is the frequency of the central node of the associated data event being facies i. By iterating over the list, the frequency of matches and central node values can be determined and used to construct ccpdf. However, exhaustive iteration of the list consumes significant CPU resources, and can be reduced through sorting grouping.

Gravey and Mariethoz (2020) propose the QuickSampling simulation algorithm (QS), designed to leverage modern hardware for fast simulation of categorical and continuous attributes. The method decomposes standard distance metrics (Manhattan and Euclidian) as sums of cross-correlations, enabling fast computation of a mismatch map using fast Fourier transforms. An optimized partial sorting algorithm is then used to quickly identify candidate patterns that are suitable for insertion into the simulation grid.

1.2.7 High-Order Simulation

The reliance of multi-point methods on the TI may result in simulations reproducing the statistics of the TI, rather than the statistics of the samples; an issue that becomes more apparent as the density of the conditioning data increases (Osterholt, 2007; Goodfellow et al., 2012). Though, the sparsity of the data may make multi-point methods suitable for the oil and gas industry, the mining industry uses substantially denser data sets that make the use of multi-point methods challenging, as multi-point methods reproduce the statics of the TI and not that of the data. Dimitrakopoulos et al. (2010) presents high-order statistics of spatial fields, enabling reproduction of high-order statistics using spatial cumulants, which provide a measure of anisotropic spatial connectivity. The relationship between the in-situ phenomena and cumulants are presented for many examples, providing an intuition between the observed behaviour of the phenomena and associated cumulants. Mustapha and Dimitrakopoulos (2010) provide an implementation for calculating experimental spatial cumulants, and provides further exploration of spatial templates, effect of data density, and the relationship between the spatial phenomena and cumulants.

Mustapha and Dimitrakopoulos (2010) introduce HOSIM, a high-order simulation algorithm using Legendre polynomials. First, a search tree is constructed, storing spatial cumulants, which are computed from the conditioning data where possible, but fall back to the TI when insufficient data is available. Then, at each simulation node, a spatial template is defined by the neighboring conditioning data and used to obtain the high-order spatial cumulants from the search tree. The spatial cumulants are then used to compute the coefficients of the Legendre series and construct a ccpdf, after which a value is then drawn from the ccpdf and added to the conditioning set. Several case studies are presented, demonstrating the methods ability to reproduce the data statistics (histogram, variogram, and higher-order statistics), and the data driven approach of the method reduces reliance on the TI, making the algorithm less sensitive to the TI than multi-point methods. Minniakhmetov and Dimitrakopoulos (2017) extend HOSIM to jointly simulate multi-variate deposits. Yao et al. (2018) provides a new computation model of computing the Legendre polynomial series using moments, improving reproduction of statistics compared to the original method as truncation Legendre series if not required.

Minniakhmetov et al. (2018) improve upon the HOSIM algorithm with Legendre like splines, improving the stability of the ccpdf approximation. Low order Legendre polynomials poorly approximate the ccpdf, while high order polynomials are unstable. Legendre like splines provide better, more stable approximations, improving the quality of simulations in terms of reproduction of statistics. De Carvalho et al. (2019) extend this method to directly simulate block values, improving the computational efficiency and memory requirements of the algorithm. Minniakhmetov and Dimitrakopoulos (2022) provide high-order sequential simulation algorithm suitable for categorical attributes based on Legendre like splines. Yao et al. (2021) provides a TI free high-order simulation method utilizing a statistical based learning method capable of inferring the ccpdf from spare drill hole data.

1.3 Strategic Mine Planning with Uncertainty

The previous sections highlight the limitations of estimated models and deterministic optimization. Many methods of generating stochastic orebody realization were presented in the previous section, providing the foundation for stochastic mine planning. In this section stochastic mine planning will be presented.

1.3.1 Managing Risk

Early methods for mine planning considering geological uncertainty focused on generating deterministic designs for a set of geological scenarios and selecting from the generated designs the one that performed best according to a predefined set of criteria. Dimitrakopoulos et al. (2007) proposes the maximum upside, minimum downside approach, where, for each geological scenario, a deterministic design is generated, and its performance assessed on all other geological scenarios. The designs are evaluated by the minimum acceptable return and upside potential. Though this method enables quantification of risk, it does not integrate and directly manage the geological uncertainty in the generation of production schedules, leading to sub-optimal designs.

Godoy (2003) proposes a multi-step process for considering geological uncertainty in production scheduling, using the notion of a stable solution domain (SSD). The SSD is defined as the area bounded between all best-case and worst-case lines on a waste-ore plot. Each best- and worst-case line combo is generated from a deterministic optimization on the respective geological scenario. The SSD defines the feasible production rates across all scenarios. Next, the optimal rate of waste and ore production are determined within the SSD, and for all geological scenarios, a production schedule satisfying the optimal production rates is generated. Lastly, the production schedules are combined into a single schedule using simulated annealing. Godoy (2004) showcases the importance of incorporating uncertainty in production scheduling, as the risk-based approach achieves a 28% increase in value compared the deterministic approach in the Femistone case study. Additionally, the case study also shows the misleading forecasts that can be obtained from deterministic mine planning. However, this is still a sequential procedure, and the last step of merging the schedules minimizes deviations from the productions rates, rather than directly maximizing NPV.

Ramazan (2004) proposes uncertainty-based production scheduling which minimizes the probability of not meeting production targets. Using a set of stochastic orebody models, each block is assigned a probability of being ore, which is used to compute Y_1^t, the deviation from 100% probability that the material mined in period t has desirable properties. The objective function minimizes the weighted sum of Y_1^t over the life of mine, with weight decreasing with time. The decreasing weight introduces the notion of a geological distribution rate, which promotes the extraction of more certain material in early periods and delays the extraction of uncertain/riskier material to later periods, when more information becomes available. Additionally, to promote smooth operational production schedules a mining width penalty is imposed, incurring a cost whenever a block is extracted in a period different than its neighbors. The case study on a Nickel Laterite deposit demonstrates the benefit of the uncertainty-based approach, compared to the traditional approach, with 6% increase in probability of achieving production targets in the first year. However, the uncertainty-based approach does not explicitly maximize NPV, rather it promotes the extraction of desirable material.

Though the previous methods provide a means of considering risk in strategic planning, none of them explicitly maximize NPV while directly considering geological uncertainty. Formulating the open pit mine production scheduling problem as a two-stage stochastic integer program (SIP) with recourse overcomes this issue (Birge and Louveaux, 2011), explicitly maximizing NPV while considering supply uncertainty. Ramazan and Dimitrakopoulos (2005); Dimitrakopoulos and Ramazan (2008); Ramazan and Dimitrakopoulos (2013) present two-stage SIPs for open pit mine production schedule, maximizing expected NPV while directly managing geological risk. The production scheduling decisions are first stage, and the second stage decisions are the deviations from targets (tonnage, grade, and metal), resulting from the production scheduling decisions (first stage). Formulating open pit mine production scheduling as an SIP provides significant benefit compared to the previous methods. The value of the stochastic solution (Birge and Louveaux, 2011) guarantees that solutions obtained from the previous methods can be no better than the production schedules obtained from the SIP, and many studies have demonstrated significant positive value (Godoy, 2004; Ramazan and Dimitrakopoulos, 2005; Leite and Dimitrakopoulos, 2007; Dimitrakopoulos and Ramazan, 2008; Ramazan and Dimitrakopoulos, 2013).

Benndorf and Dimitrakopoulos (2013) present a SIP for optimizing open pit mine production schedules under joint multi-element uncertainty. The formulation also includes a term for penalizing highly selective schedules, promoting smoother more operationally feasible extraction sequences. The case study showcases the methods ability to provide optimized production schedules which maintain grades within tight windows. The case study also explores the effect of selectivity, providing three cases generated with different smoothness penalties. Generally, compliance to production targets becomes more strained as the smoothness penalty increases. However, appropriately tuned smoothness penalties are able to produce smooth schedules, which provide adequate compliance to production targets.

Menabde et al. (2018) provides stochastic mixed integer program (MIP) formulation for jointly optimizing production schedules and cut-off grades under supply uncertainty. The MIP does not contain any second stage or recourse variables, instead the production constraints are enforced through chance constraints, which must be satisfied for a certain proportion of the scenarios. The decision variables represent the decision to mine selective mining unit i under cut-off grade j in period t, requiring that a set of pre-defined cut-off grades be provided. As a result, the quality of the cut-off grade optimization is highly dependent on quality of the provided cut-off grade discretization. The provided case study demonstrates 20% increase in value when the schedule and cut-off grade are jointly optimized. Similarly to cut-off grades from Lane's method, the cut-off grade starts high and trends downward over the life of the mine.

Quigley et al. (2018) simulates rare earth elements and optimizes the life of asset production schedule and destination policy of blocks. First, the domains are simulated using SNESIM, then block grade values are simulated with DBMAFSIM. The life of asset production schedule and destination policy are then optimized, maintaining strict product quality requirements. The proposed method increases the NPV by 12% compared to the conventional base case comparison.

Macneil and Dimitrakopoulos (2017) propose a method stochastically optimizing the transition from open pit mining to underground operations. The method requires a set of candidate crown pillars, which defines the maximum depth of the open pit. For each candidate location, the open pit is stochastically optimized (Ramazan and Dimitrakopoulos, 2013), followed the underground operations, using a similar formulation with modified precedence constraints for UG. The best transition depth is selected as the one which maximize the combined NPV from both the UG and open pit operations.

Dimitrakopoulos and Jewbali (2013) proposes a multi-step method for optimizing short- and long-term production schedules, incorporating grade control data. First, high density future grade control data is simulated using exploration data and grade control data from previously mined out areas. Exploration models are updated using simulation by successive residuals (Vargas-Guzmán and Dimitrakopoulos, 2002), and stochastic optimization is re-performed on the updated models. Incorporation of grade control data provides short scale information, not captured by the widely spaced exploration data, potentially leading to better reconciliation. In the presented case study, the method provides better forecasts that more closely match the mines reconciliation.

Khan and Asad (2019) provide a stochastic cut-off grade optimization method, considering the uncertain supply of material. The method provides an optimal cut-off grade schedule over the life of mine (LOM), maximizing NPV. Similar to Menabde et al. (2018), a grade binning approach is used to discretize the space of all possible cut-off grades. The first stage decisions represent the quantity of material to extract from grade bin b and send to destination d. However, the method does not consider stockpiling or multiple elements.

Two-stage SIPs, like those discussed above, provide no means of adapting to realizations of outcomes of the unknown parameters (grade, equipment availability, commodity price, etc.). However, mine planning defines a sequence of decisions over time, and decisions that occur latter in time can react to realizations of outcomes that result from decisions made earlier in time. Multi-stage stochastic programming provides the model for optimal decision-making in this setting (Birge and Louveaux, 2011). Boland et al. (2008) provides multi-stage stochastic programs for optimizing open pit mine production schedules under geological uncertainty. The first formulation provides scenario dependent processing decisions, while the second formulation includes scenario dependent mining decisions. Both formulations include non-anticipativity constraints, which ensure that the same decisions must be applied when the scenarios cannot be distinguished. However, the formulation requires some strong assumptions which are not reasonable in practice. One such assumption is the grade order preserving assumption which assumes that selective mining unit (SMU) i has a grade higher than SMU j in simulation s, then that relationship holds in simulation r. Additionally, multi-stage production scheduling poses a significant computational challenges, requiring aggregation to maintain tractability.

All methods discussed in this section directly integrate and manage risk associated with geological uncertainty, presenting a significant advantage over deterministic counterparts. However, they are all based upon the economic value of blocks, and lack in their ability to model and optimize for the true value of products sold.

1.3.2 Simultaneous Stochastic Optimization

Unlike the methods discussed in the previous section, where economic values of blocks drive the optimization, simultaneous stochastic optimization (SSO) maximizes the value of products sold considering all components of a mining complex (Montiel and Dimitrakopoulos, 2015; Goodfellow and Dimitrakopoulos, 2016; Montiel et al., 2016; Goodfellow and Dimitrakopoulos, 2017; Montiel and Dimitrakopoulos, 2017; 2018). Generally, a mining complex models material supply, stockpiles and storage, value adding transformative nodes, transportation, markets, and clients. The flexibility of SSO enables all relevant components to be modelled, capturing all transformative actions applied to mined material. The transformations may take any form and need not be linear.

Simultaneous optimization of entire mining complexes enables exploitation of the relationship between various internal components. For example, if multiple mines feed the same processing facility, simultaneous optimization would advantageously blend material from the mines to provide the optimal blend to the mill. However, sequential optimization would be unable to capture this synergy as each mines schedule would be optimized in isolation from the other. By exploiting relationships between various mining complex components, higher value solutions that better satisfy production targets can be obtained.

Montiel and Dimitrakopoulos (2013) stochastically optimize a mining complex using a sequential approach, similar to (Godoy, 2004). First, an initial solution is generated, then using simulated annealing, the solution is improved, minimizing deviations from targets. The perturbations can affect the schedule, and destination of blocks. However, if the material classification of a block is not constant across all provided scenarios, the destination is not perturbed to avoid material misclassification issues. An application of this method on Escondida Norte shows significant improvement in deviations from targets. Additionally, even though this method does not directly maximize NPV, the case study demonstrates a 4% increase in NPV. However, this method is not a true simultaneous approach, and further improvements can be obtained with better destination policies and directly maximizing NPV.

(Montiel and Dimitrakopoulos, 2015); Montiel et al. (2016); Montiel and Dimitrakopoulos (2017; 2018) extend the previous method, formulating an SIP that maximizes NPV and minimizes deviations from targets. The NPV is calculated from the value of products sold and the costs incurred, rather than economic block values, enabling blending and material transformations to be exploited. Simulated annealing is used to solve the SIP, with three main classes of perturbations. Block perturbations may change the period and or destination of block, operating based perturbations effect the operating mode at processing nodes (ex: fine vs coarse grinding), and transportation-based perturbations effect utilization of possible transportation streams at output nodes. Simultaneously considering all these components under a single mathematical formulation enables synergies to be leveraged, increasing NPV and decreasing deviations. A case study at a mining complex consisting of two pits and 5 processing stream destinations shows significant improvement in deviations from targets and increases in NPV (Montiel and Dimitrakopoulos, 2015). An application the Nevada’s Twin Creek mining complex finds a 7% increase in NPV over the LOM, 6% increased recovered gold, and reduced deviations from targets (Montiel and Dimitrakopoulos, 2018).

Goodfellow and Dimitrakopoulos (2016; 2017) propose a two-stage SIP for simultaneously optimizing mining complexes. The first stage decisions define the extraction sequence and the destination policy, and second stage decisions control the downstream flow of material. A meta-heuristic is used, enabling optimization of exceptionally large problems (millions of blocks over 20+ years) and modeling of non-linear material transformations. The formulation defines two types of properties: (1) primary, which are additive and may be transferred between nodes, and (2) hereditary, which are defined as functions of primary attributes and need not be additive. Previously, primary attributes have been well addressed in literature, however, the complexities of dealing with non-linearity has resulted in hereditary attributes largely being ignored. The proposed metaheuristic efficiently handles non-linearities imposed by the hereditary properties, allowing modeling and optimization of entire mining complexes, focusing on the value of products sold, rather than economic block values.

Goodfellow and Dimitrakopoulos (2016) proposes a cluster-based destination policy suitable for multiple elements in the presence of uncertainty. Under the cluster-based destination policy, the destination of a block is scenario dependent and defined by the cluster to which it belongs. The cluster membership is defined by the block's properties in each scenario. Using k-means++, k centroids are defined, and in each scenario a block is assigned to the nearest cluster centroid. The locations of the centroids are optimized such that the within cluster similarity and the out of cluster dissimilarity are maximized. The number of clusters k is required as input, and the algorithm will define the location of k centroids, assigning each block to the cluster associated to its nearest centroid. Destinations can then be assigned to each centroid, enabling blocks to be sent to different locations in different scenarios depending on their properties. Such a destination policy is effective for multiple elements under supply uncertainty. However, the resulting policy is difficult to interpret, as determining the destination of a block requires first determining the cluster to which it belongs, and then identifying the destination of that cluster in the period of interest. Identifying the cluster to which a block belongs requires finding the nearest cluster centroid, which is not a trivial task. Compared to a cut-off grade policy, where a blocks destination can be determined by simply comparing its properties to the cut-off thresholds, the cluster-based policy introduces additional complexity making operational use difficult. Mult-element cut-off grades provide a more operationally usable destination policy; however, no previous research has explored optimizing multi-element cut-off grade policies under uncertainty with multiple destinations.

Capital expenditures are a challenging component of simultaneous stochastic optimization of mining complexes. Typically, capital expenditures are predefined, and not included in the optimizer. However, the value of a mining complex and how it operates is dependent on capital expenditure decisions as they effect mining rates, processing rates, transportation, tailings capacity, etc. Thus, optimizing capital expenditures simultaneously with all other components of a mining complex desirable.

Goodfellow (2014) incorporates CAPEX decisions for increasing or decreasing production. The CAPEX decisions are incorporated into the formulation presented in (Goodfellow and Dimitrakopoulos, 2016) as first stage decisions. The formulation incorporates lead-times and CAPEX timing constraints to ensure feasible CAPEX decisions. An application of the method on a copper mining complex, with CAPEX for increasing mining rates through the purchase of trucks and shovels demonstrates a 5.7% increase in NPV compared to a deterministic equivalent.

Farmer (2016) extends (Goodfellow and Dimitrakopoulos, 2016) to optimize CAPEX decisions in the pre-production stage, incorporating metal price uncertainty into downstream decisions, and financial contract based revenues. The formulation is applied to a copper-gold mining complex, showing an 11% improvement in NPV compared to a stochastic optimization with fixed capacities. The milling capacity was modelled as a one-time CAPEX decision executed in the first year, with a 2-year lead time, and the mining capacity CAPEX decision could be made throughout the LOM but had a 2-year lead-time.

Zhang and Dimitrakopoulos (2017) develop a decomposition method for optimizing mining complexes. The method first optimizes the production schedule, defining the tonnages of each material type available, then the down stream decisions are optimized. The down stream optimizer can buy or sell material, which is used to update the value of each material type. If material is sold, then the schedule provided to much of it and its value is decreases, whereas if material is purchased, the schedule didn't provide enough, and its value is increased. The production schedule is then reoptimized and the process is iteratively repeated until the value update is sufficiently small. Application of the method on a mining complex consisting of two copper mines, stockpiles, and 15 material types yielded a 6% improvement in NPV compared to local optimization approach.

Del Castillo and Dimitrakopoulos (2019) develops an adaptive simultaneous stochastic optimization framework for optimizing mining complexes, considering feasible CAPEX decisions. The method allows the solution to branch if a representative number of scenarios makes the same CAPEX decision, allowing the mining complex to adapt to uncertainty as it is revealed. Requiring a representative number for branching prevents overfitting to the scenarios. Once a scenario branches, all previous decisions are fixed, enabling a mine plan to be followed through the LOM. A case study on a copper mining complex, with CAPEX decisions for purchasing trucks, shovels and a secondary crusher is presented. Branching is enabled for the decision to purchase a secondary crusher, allowing for specialized mine plans able to fully utilize the available capacity. The case study finds a 3% increase in NPV compared to the base case 2-stage SIP without branching.

1.3.3 Smarter Solvers for Simultaneous Stochastic Optimization of Mining Complexes

Simultaneous stochastic optimization of mining complexes is computationally challenging, often requiring millions of binary decision variables, with non-linear transfer functions, and complex constraints. Smarter more capable optimization algorithms provide higher quality solutions in a shorter amount of time, enabling more complex formulations, considering more aspects of a mining complex.

Lamghari and Dimitrakopoulos (2012) optimizes mine production schedules with diversified Tabu search. Two diversification strategies are used; a long term memory approach which moves blocks into period in which they are less frequently scheduled, and a variable neighborhood approach based on (Hansen and Mladenović, 2001). The long-term memory diversification approach was found to perform better than the variable neighborhood approach on larger problems.

Lamghari et al. (2014) presents variable multi-neighborhood descent for optimizing open pit mine production schedules. The neighborhoods are defined: swap, which selects two blocks and swaps their periods, shift after, delaying the extraction of a block, and shift before, accelerating the extraction of a block. Each neighborhood is exhaustively searched until no more improving perturbations are found, in an iterative procedure until no improving moves exist in all three neighborhoods. The method requires an initial solution but is not sensitive to the quality of the solution.

Lamghari and Dimitrakopoulos (2020) proposes three hyper heuristics and compares their performance. The first hyper heuristic keeps scores for low-level heuristics and uses reinforcement learning principles to select low-level heuristics and update their scores. The second hyper heuristic employs a more sophisticated scheme for selecting and updating heuristics. The third hyper heuristic utilizes a scoring scheme which incorporates the heuristics effect on objective function value and it's time, and selects low-level heuristics probabilistically based on its score. The third hyper-heuristic was found to perform best, with an average gap from the linear relaxation of 0.79% compared to 35.1% for the first and 48.34% for the second heuristic.

Reinforcement learning (RL) (Sutton and Barto, 2018) is a machine learning approach aimed at solving sequential decision-making problems in complex and uncertain environments. It operates by training an agent to make decisions that maximize long-term cumulative rewards based on interactions with the system. In mining optimization, RL presents a flexible methodology for addressing challenges such as resource allocation and scheduling, where traditional optimization methods may struggle to adapt to the system's evolving nature. By continuously refining its strategy through feedback, RL enables more efficient exploration of possible solutions, particularly in highly dynamic and stochastic contexts.

Yaakoubi and Dimitrakopoulos (2023) proposes the learn-to-perturb hyper heuristic, which learns the best low-level heuristics to apply in different problem states. The sampling of the low-level heuristics is biased by the performance on the heuristic in previous iterations, with more performant heuristics being favored. The score of each low-level heuristic is a combination of its performance and weighting according to an agent. Testing on several mining complex instances with multiple RL agents, learn-to-perturb hyper heuristic was found to reduce computation time by 80%.

1.4 Goal and Objectives

The goal of the research presented in this thesis is to further develop and incorporate operational components in stochastic strategic mine planning. To this end, joint stochastic optimization of long-term production schedules with ramp design while ensuring equipment access to scheduled blocks and optimizing multi-element cut-off grades under geological uncertainty for optimal production plans are explored in detail. The following objectives are set to meet this goal:

- Review the technical literature related to open pit mine production scheduling with ramp design, cut-off grade optimization, deterministic and stochastic methods for strategic mine planning, and geostatistical simulation methods.
- Examine geostatistical simulation methods for incorporating geological uncertainty into the mine planning process
- Develop a stochastic optimization model for jointly optimizing open pit mine production schedules and ramp design considering geological uncertainty.
- Develop a reinforcement learning framework for optimizing multi-element cut-off grades under supply uncertainty given an optimal production schedule.

1.5 Thesis Outline

This thesis is organized into the following chapters.

Chapter 1 presents a review of the literature related to deterministic and stochastic mine planning, joint production schedule and ramp design, cut-off grade optimization, and geostatistical simulation methods.

Chapter 2 presents a stochastic integer program for jointly optimizing long-term open pit mine production schedules and ramp under geological uncertainty. An application at a gold mine is presented demonstrating the methods ability to generate feasible production schedules that meet production targets while managing risk.

Chapter 3 presents reinforcement learning framework for optimizing multi-element cut-off grade under supply uncertainty for an optimal production schedule. Application at a gold-copper mine demonstrates the methods ability to generate cut-off grade policies that meet target production forecasts under supply uncertainty.

Chapter 4 summarizes the contributions in the previous chapters and overall conclusions and presents suggestions for future work.

Chapter 2. Joint Stochastic Optimization of Open Pit Mine Production Scheduling with Ramp Design

2.1 Introduction

Open pit mining is a large-scale extractive activity in which substantial quantities of material are excavated from a continually expanding pit and transported for further treatment. The transportation of mined material from its point of excavation to its next destination requires a road and ramp network, connecting mining locations to material destinations (Hustrulid et al., 2013). Ramps are usually placed adjacent to the pit wall and enable equipment to travel between benches, while roads enable equipment to traverse across flat terrain, such as a bench, or from the pit exit to the crusher. Typically, the ramp and road network are designed after the long-term production schedule has been optimized, as the schedule defines when and where equipment access is required. However, ramps and haul roads are relatively large pieces of infrastructure which not only effect the geometry of the pit defined by the long-term schedule, but also the availability of material. The modifications required to accommodate a ramp and road network can decrease the performance of the long-term schedule, decreasing net present value (NPV). As a result of the co-dependence between the ramp and road design, sequential optimization of either component individually can lead to sub-optimal results. In this work, the joint optimization of the long-term production schedule and ramp and road design while ensuring feasible equipment access to scheduled mining blocks is proposed, to address the issues arising from the sequential process.

Conventionally, open pit mine production schedules are formulated deterministically, however, orebodies are heterogenous, and a single smooth estimate of the orebody provides no information about the variability and uncertainty of the material in the ground. Stochastic optimization for open pit mine production scheduling improve upon their deterministic counterparts by taking as input a set of geostatistical simulations (Goovaerts, 1997), which represent the variability and uncertainty of material in the ground. Ramazan and Dimitrakopoulos (2005) first proposed a two-stage stochastic integer program for open pit mine production scheduling, which was limited to a single element mine with-out a stockpile. The value of the stochastic solution as it relates to mine production scheduling was then demonstrated in Dimitrakopoulos and Ramazan (2008). Since then, stochastic formulations for mine planning have been extended to include stockpiles

(Ramazan and Dimitrakopoulos, 2013), multiple elements (Benndorf and Dimitrakopoulos, 2013; Quigley et al., 2018), and entire mining complexes (Goodfellow, 2014; Montiel and Dimitrakopoulos, 2015; Goodfellow and Dimitrakopoulos, 2016; 2017; Montiel and Dimitrakopoulos, 2018). Simultaneously optimizing entire mining complexes in the presence of uncertainty increases values, improves forecasts, and reduces risk (Goodfellow, 2014; Montiel and Dimitrakopoulos, 2015; Goodfellow and Dimitrakopoulos, 2016; Montiel et al., 2016; Goodfellow and Dimitrakopoulos, 2017; Montiel and Dimitrakopoulos, 2018; Kumar and Dimitrakopoulos, 2019; Dimitrakopoulos and Lamghari, 2022). Concurrently, the optimization of large stochastic problem has been extensively studied, leading to the development of many advanced heuristic methods (Lamghari and Dimitrakopoulos, 2012; Lamghari et al., 2014; Lamghari and Dimitrakopoulos, 2020; 2022), and smart solvers leveraging reinforcement learning (Yaakoubi and Dimitrakopoulos, 2023) . However, in all past approaches, block access is defined solely through the slope constraints, and does not explicitly consider the ramp and road network required to facilitate equipment access to the scheduled mining blocks. As a result, the optimized production schedules require modification to accommodate the placement of ramps and roads, while ensuring feasible equipment access to scheduled mining blocks, affecting the value of the previously optimized solution.

Previous work to optimize ramp and road design considers it to be separate from open pit mine production scheduling and has focused on optimizing ramp design for a predefined ultimate pit limit (UPL). Gill (1999) provides a dynamic programming approach, which optimizes the ramp design for a given ultimate pit limit. The dynamic program discretizes ramps into single bench segments and identifies the combination of segments providing access from the surface to the lowest bench, while considering the cost of stripping additional material (expanding the predefined pit) and leaving material unmined (shrinking predefined pit). Nancel-Penard et al. (2019) propose a method which, takes as input a set of pre-defined pushbacks, and generates an optimal ramp design considering the cost of additional blocks to be extracted, while also modifying the pushback design to provide space for ramp placement. Yarmuch et al. (2020) optimize the design of both the ramp within the pit, and the ex-pit haul road, considering construction, haulage and maintenance costs. The ex-pit haul roads are optimized using a shortest path approach, while the ramp design is optimized via a binary linear program, which minimizes the ramp costs. Morales et al. (2023) develop a mathematical program which optimizes the discretized pushback design, while ensuring adequate space between pushbacks for ramp placement and then uses an algorithm to construct an operational push back design. However, in all previously presented methods the schedule is not informed by the placement of ramps and the accessibility which it provides. In an operating mine, equipment requires road access to all scheduled mining activities, meaning that mining is required to progress outwards from the ramp. The co-dependence of the schedule and ramp/road design means that any optimization process which does not jointly consider both the schedule, and the ramp design results in a sub-optimal solution that does not leverage the relationship between the two components. In this study, the goal is to introduce a novel approach for jointly optimizing open pit mine production scheduling and ramp design. Accordingly, a two-stage stochastic integer program (SIP) (Birge and Louveaux, 2011) for optimizing long-term open pit mine production schedules while ensuring equipment access through ramps and road is presented. This differs from previous methods in that scheduling and ramp design are jointly considered under one mathematical formulation, rather than considering them separately in a stepwise approach as done in previous studies. The SIP builds upon the formulation presented in Ramazan and Dimitrakopoulos (2013) to ensure feasible equipment access by requiring that all mined blocks be accessible from a road that leads to the top of the pit in the period in which they are mined. Roads are modelled as two separate components; intra-bench roads which facilitate traversal across benches, and ramps which facilitate traversal between benches similarly to Gill (1999). Intra-bench roads are constructed such that they join ramps to a set of predefined locations on each bench called checkpoints, and a block is considered accessible from that road if it is within the checkpoints window. Formulation of the SIP requires the set of all checkpoints, ramps and intra-bench roads to be predefined, which may be achieved through the pre-processing procedure presented below.

In the following section the preprocessing procedures and proposed stochastic mathematical program are first presented. Next, the method is applied to a gold mine and results are discussed. Conclusions and directions for future work follow.

2.2 Method

This section presents a stochastic mathematical program which jointly optimizes the long-term open pit mine production schedule and ramp design under grade uncertainty, while ensuring feasible equipment access to scheduled mining blocks. First, checkpoints, ramps and intra-bench roads are discussed in more detail. Then, the notation, constants, sets, and variables are presented, followed by the SIP.

2.2.1 Checkpoints

Checkpoints are regularly spaced nodes, which, when active provide access to all mining blocks within their window. For a checkpoint to be active, there must exist a road connecting it to the top of the pit. An example of an active checkpoint is provided in Figure 2-1, where an isometric view of a bench containing a checkpoint, road, and ramp is shown. The sphere represents the checkpoint node, and the shaded rectangular prism denotes the area which the checkpoint provides access to. The arrow represents the path through which a road may progress to reach and activate the checkpoint.

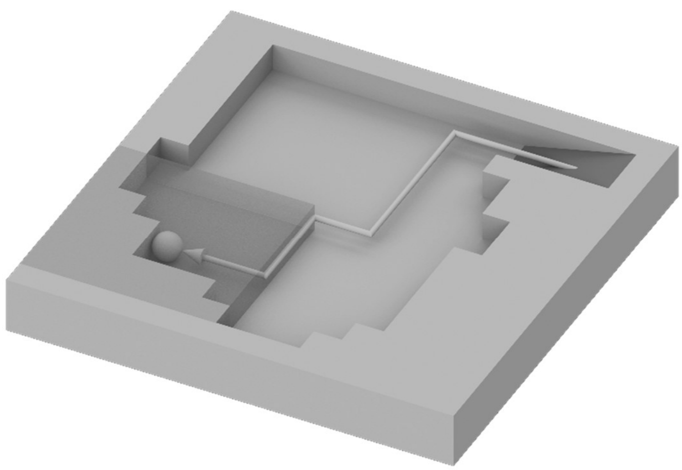

Figure 2-1: Isometric view of a bench depicting a checkpoint (sphere), accessible blocks (shaded volume), road (arrow) and ramp.

2.2.2 Ramp Segments

Ramp segments are single bench ramps, modeled as a collections of mining blocks which approximate the true shape of the ramp. Modeling ramp segments as a collection of mining blocks allows ramp design decisions to be easily translated to the schedule and mining blocks which they effect. To fully define a ramp the following components are required; location (i): index of the block at the top of the ramp, period (t): Time period when the ramp is present, and design (d): Set of blocks contained in the ramp.

2.2.3 Intra-bench Roads

Intra-bench roads define the set of blocks connecting two points on the same bench and are modeled as the composition of sub- and super-roads. Sub-roads are short high resolutions paths, joining adjacent checkpoint nodes, while super-roads are long low-resolution paths joining blocks at large distances. Figure 2 shows an isometric view of a bench, with checkpoints, sub-roads, and a super road. Sub-roads define the exact set of blocks through which the road progresses, while super roads define the general area through which a road must progress. In Figure 2-2, the super-road provides access to the bottom left most checkpoint, and the super-road may be traversed by any of the sub-roads connecting the checkpoints through which the super-road progresses. Modeling intra-bench roads as the composition of these two components reduces the number of decisions variables required in the stochastic mathematical program, while still providing multiple access strategies, as the sub-road network provides multiple ways of traversing each super-road.

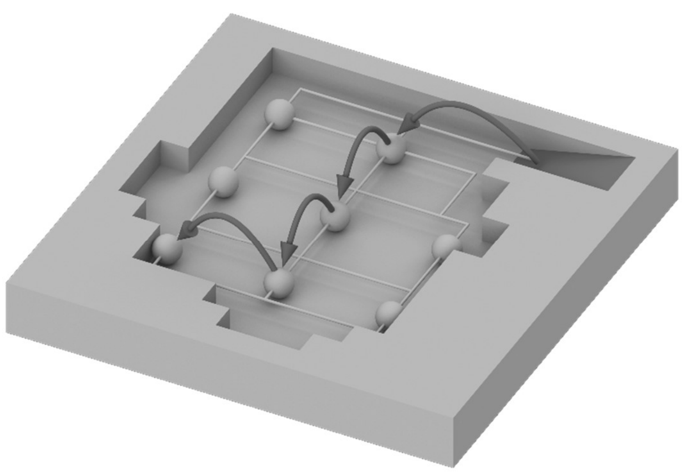

Figure 2-2: Isometric view of a bench depicting checkpoints (spheres), sub-roads (grid of arrows), and a super-road (curved arrow).

2.2.4 Road and Ramp Generation

Automatic generation of both ramps, and intra-bench roads can be achieved using a graph traversal algorithm with unique stopping criteria to identify when a ramp/intra-bench road has been generated. Here, depth first search (DFS) (Knuth, 1997) is used as the traversal algorithm, which starts at a defined initial location and constructs a path by recursively adding/removing extensions to the current path at each recursive step. Extensions to the path are generated such that they maintain the desired path width, and satisfy any operational constraints such as turning radius, length, complexity, etc. Maximum road grade can be enforced by ensuring that all ramp segments exceed a minimum required centerline length. An example of automatic path generation through DFS is provided in Figure 2-3, where path extensions (orange) are added to the path, and fill blocks are inserted (yellow) as required to maintain path width. Switch backs may be constructed by combining multiple segments across benches.

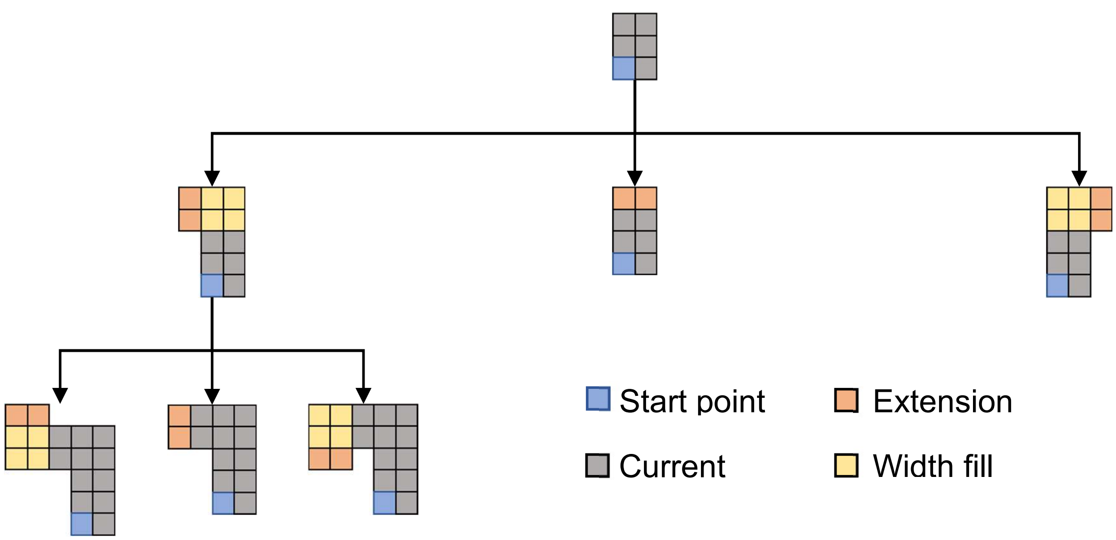

Figure 2-3: Ramp and road generation tree. The children of each node compose the set of all possible roads that can be constructed by adding a single extension.

2.2.5 Definitions and Notation

The tables in this section present the indices, sets, constants and variables used to define the proposed SIP. Table 2-1 presents the index notation, while Table 2-2 contains all sets of variables used throughout the formulation. Table 2-3 and Table 2-4 present the constants and variables, respectively.

Table 2-1: Indices.

i	Mining block index
s	Simulation index
t	Period
d	Ramp design index
j	Check point index
k	Super-road index
l	Sub-road index
g	Super-road segment index

Table 2-2: Sets.

$CPI(i)$	Set of checkpoints with windows overlapping block i
$ADJ^R(k)$	Set of ramps (described by their location i, and design d) which terminate adjacent to the beginning of super road k
$PRED(i,d)$	Set of predecessor blocks for ramp located at i, with design d
$XSEC(i,d)$	Set of ramps intersecting ramp at location i, with design d
$SEG(k)$	Set of segments composing super-road k
$ADJ^{s-}(g)$	Set of sub-roads traversing super-road segment g
$ADJ^{s+}(j)$	Set of super-roads adjacent to checkpoint j
S	Set of simulations
I	Set of mining blocks
T	Set of years
D	Set of ramp designs
K	Set of super-roads

L	Set of sub-roads
J	Set of checkpoints

Table 2-3: Constants.

$v_{i,s}^{t}$	Economic value of block i in period t for scenario s
rc^{t}	Cost of placing or removing a ramp in period t
$c_{o}^{t-,+}$	Penalty cost for deviating below $(-)$ or above $(+)$ ore target
$c_{g}^{t-,+}$	Penalty cost for deviating below $(-)$ or above $(+)$ metal target

Table 2-4: Variables

b_{i}^{t}	Binary	Mine block i period t
$r_{i}^{t,d}$	Binary	Ramp with design d exists at i period t
$\check{r}_{i}^{t,d}$	Binary	Ramp with design d placed/removed at i in period t
cp_{j}^{t}	Binary	Checkpoint j is active in period t
s_{k}^{t+}	Binary	Super-road $k \in K$ is active in period t
s_{l}^{t-}	Binary	Sub-road $l \in L$ is active in period t
d_{s}^{to-}, d_{s}^{to+}	Continuous	Deviation below/above target for ore tonnage in scenario s in period t
d_{s}^{tg-}, d_{s}^{tg+}	Continuous	Deviation below/above target for grade in scenario s in period t

2.2.6 Stochastic Integer Program

2.2.6.1 Objective Function

The objective function, shown in Equation 1 consists of 3 main parts. Part 1 maximizes the discounted cumulative cashflow of the extraction sequence, Part 2 incurs the cost of placing and removing ramps over the life of the mine, and Part 3 penalizes deviations from grade and ore tonnage targets. Part 1 and Part 3 are identical to the objective function described in Ramazan and Dimitrakopoulos (2013) without stockpiling.

$$\underbrace{max\frac{1}{|S|}\sum_{s\in S}\sum_{i\in I}\sum_{t\in T} b_i^t v_{i,s}^t}_{Part\ 1} - \underbrace{\sum_{i\in I}\sum_{t\in T}\sum_{d\subset D} \mathrm{rc}^t \check{r}_i^{t,d}}_{Part\ 2} \tag{1}$$
$$\underbrace{\frac{1}{|S|}\sum_{s\in S}\sum_{t\in T}(c_o^{t-}d_{so}^{t-} + c_o^{t+}d_{so}^{t+} + c_g^{t-}d_{sg}^{t-} + c_g^{t+}d_{sg}^{t+})}_{Part\ 3}$$

2.2.6.2 Constraints

The following sub-sections present the constraints of the stochastic mathematical program, which when combined ensure equipment access to scheduled mining blocks.

Ramp Placement/Removal Constraints: The ramp placement/removal constraints in Equations 2 and 3 ensure ramp placement/removal variables are greater than zero whenever a ramp is placed or removed, storing the absolute value of $r_i^{t,d} - r_i^{t-1,d}$ in $\check{r}_i^{t,d}$, which incurs a cost in the objective function.

$$\check{r}_i^{t,d} \geq r_i^{t,d} - r_i^{t-1,d}\ \forall\ i \in I, t \in T, d \in D \tag{2}$$

$$\check{r}_i^{t,d} \geq r_i^{t-1,d} - r_i^{t,d}\ \forall\ i \in I, t \in T, d \in D \tag{3}$$

Checkpoint Accessibility Constraint: The checkpoint accessibility constraint in Equation 4 ensures that a block may only be mined if it is within the window of an active checkpoint. Since a block may be within the window of multiple checkpoints the activation state of all intersecting checkpoints must be summed, which is achieved by summing over all $cp_j^t\ \forall\ j \in CPI(i)$. Figure 2-4 shows a cross-section view of a bench with a ramp, checkpoint, and accessible blocks, providing a visual representation of the constraint. The checkpoint represented by the hatched square has a window size of 5, providing access to all blocks annotated with hatched circles. Since the two blocks to the right of the checkpoint have already been mined the only blocks available for mining are the two to the left of the checkpoint.

$$b_i^t \leq \sum_{j \in \mathrm{CPI}(i)} \mathrm{cp}_{\mathrm{j}}^{\mathrm{t}} \ \forall\, i \in I, t \in T \tag{4}$$

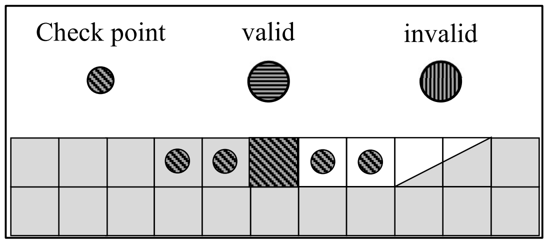

Figure 2-4: Bench cross-section containing a ramp, checkpoint (hatched square), mined blocks (white), unmined blocks (shaded), and accessible blocks (hatched circles).

Ramp Location Accessibility Constraint: The ramp location accessibility constraint in Equation 5 requires that ramps only be present where the start of the ramp is directly under an accessible location. By ensuring ramps are only placed under accessible blocks, a traversable road from the top of the pit to all ramps can be guaranteed in all periods. Since a start of a ramp may be under multiple checkpoint windows, the state of all checkpoints with windows intersecting the location directly above the start of the ramp (i^-) must be summed. In Figure 2-5, depicting the cross section of a bench, the vertically hatched ramp is valid because it starts directly below an accessible location, while the horizontally hatched ramp is invalid because it starts directly below a block that is not within the window of an active checkpoint.

$$r_{i,\,d}^t \leq \sum_{j \in \mathrm{CPI}(i^-)} \mathrm{cp}_j^t \,\forall\, i \in I,\ t \in T,\ d \subset D \tag{5}$$

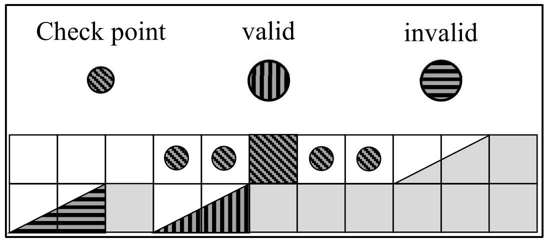

Figure 2-5: Bench cross-section of accessible and in-accessible ramp placement. Vertically hatched ramp is accessible and horizontally hatched ramp is inaccessible.

Ramp Placement Constraint: The ramp placement constraint in Equation 6 ensures that ramps are both placed in and underlain by solid material. This constraint is modelled by requiring all blocks associated with active ramps to be unmined by the period in which the ramp is present.

$$\sum_{\tau=1}^{t} \sum_{i' \in d} b_{i'}^{\tau} \leq |d| * \left(1 - r_{i,d}^{t}\right) \; \forall \, t \in T, \; i \in I, \; d \subset D \tag{6}$$

Ramp Predecessor Constraint: The ramp predecessor constraint in Equation 7 ensures that ramps may only be present if their predecessors are mined. Since ramps contain multiple blocks, the predecessors of all blocks within the ramp must be mined to ensure that slope constraints are not violated. In the bench cross-section depicted in Figure 2-6, the vertically hatched ramp is valid because all blocks in its predecessor set are mined, while the horizontally hatched ramp is placed below unmined blocks making it invalid.

$$\sum_{\tau=1}^{t} \sum_{i^* \in \mathrm{PRED}(i,\, d)} b_{i^*}^{\tau} \geq |\mathrm{PRED}(i,d)| * r_{i,d}^{t} \; \forall \, i \in I, \; t \in T, \; d \subset D \tag{7}$$

\

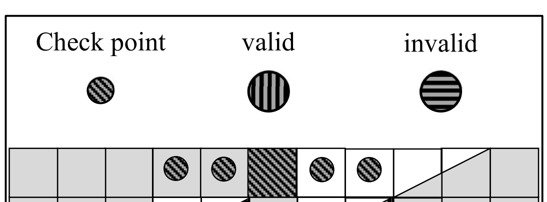

Figure 2-6: Bench cross-section of valid (vertically hatched) and invalid (horizontally hatched) ramp placements.

Ramp Intersection Constraint: The ramp intersection constraint in Equation 8 prevents two intersecting ramps from being present in the same period. In the bench cross-section shown in Figure 2-7, the placement of both ramps is invalid because they share a block, meaning they are intersecting.

$$\sum_{(i^*,\, d^*)\in \mathrm{XSEC}(i,\, d)} r_{i^*,\, d^*}^{t} \leq 1 - r_{i,d}^{t} \; \forall \; t \in T, \; i \in I, \; d \subset D \tag{8}$$

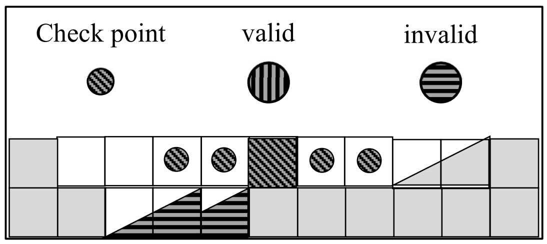

Figure 2-7: Bench cross-section with intersecting ramp placements.

Super-road Ramp Adjacency Constraint: The super-road ramp adjacency constraint in equation 9 ensures that all valid super-roads are adjacent to the end of a ramp, which is one of the three basic traverasbility requirements discussed above. To model this constraint the variable associated with the super-road must be less than or equal to the sum of all ramp variables associated to ramps that terminate adjacent to the beginning of the super-road. In the bench cross-section presented in Figure 2-8, the solid super-road is valid because it begins adjacent to the end of a ramp, while the dashed super-road is invalid because no ramp terminates adjacent to the start of the road.

$$\sum_{(i,\, d)\in \mathrm{ADJ^R}(k)} r_{i,\, d}^{t} \geq s_{k}^{t+} \; \forall \; t \in T, \; k \in K \tag{9}$$

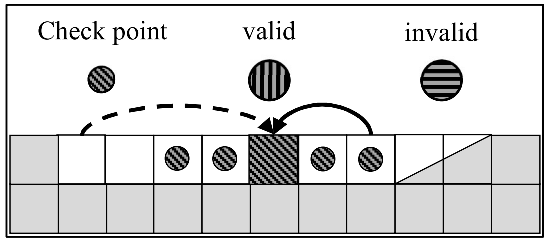

Figure 2-8: Bench cross-section with valid (solid) and invalid (dashed) super-roads.

Active Sub-Road Constraint: The active sub-road constraint in Equation 10 ensures that active roads are unobstructed and underlain by solid material. This constraint can be formulated by summing the mining decisions for blocks in the path and subtracting mining decisions for blocks directly below the path. If the expression is equal to the length of the path, then the path must be unobstructed and underlain by solid material, meaning the road may be active. If the expression has a value less than the length of the path, it is either obstructed, not underlain by solid material, or both. In Figure 2-9, a plan view of a bench, containing a ramp, checkpoints, and sub- and super-roads is depicted and serves as a visual aid for explanation of the following constraints. The sub-roads denoted by the solid black arrows are valid because they progress through mined blocks, and are entirely underlain by solid material, however, the dotted-grey sub-roads are invalid because they progress through unmined blocks.

$$\sum_{i \in l} \sum_{\tau=1}^{t} b_i^{\tau} - b_{i^+}^{\tau} \geq |l| * s_l^{t-} \ \forall \, l \in L, \, t \in T \tag{10}$$

Active Super-Road Constraint: The active super-road constraint in Equation 11 ensures that each segment of an active super-road is traversable by at least one active sub-road. The constraint can be formulated by ensuring that for each segment of the super-road, the super-road variable is less than or equal to the sum of active sub-roads traversing the segment. In the bench plan-view provided in Figure 2-9, the super-road denoted by the set of contiguous red arrows is valid because each segment (individual red arrow) of the super-road can be traversed by at-least one valid sub-road (black arrow).

$$\sum_{l \in ADJ^{s-}(g)} s_l^{t-} \geq s_k^{t+} \quad \forall g \in \mathrm{SEG}(k), \, t \in T, \, k \in K \tag{11}$$

Active Checkpoint Constraint: The active checkpoint constraint in Equation 12 ensures that checkpoints are only active in the periods in which they may be accessed through a valid haul road. The constraint is formulated by ensuring that the sum of all variables associated to super-roads that intersect that the checkpoint is greater than or equal to the variable associated to the checkpoint.

$$\sum_{k \in \mathrm{ADJ}^{s+}(j)} s_k^{t+} \geq cp_j^t \;\forall\, j \in J,\; t \in T \tag{12}$$

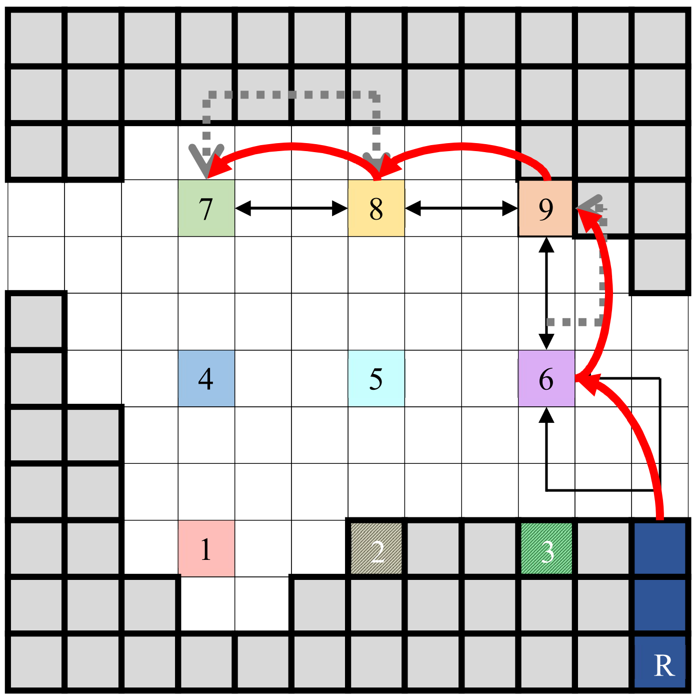

Figure 2-9: Plan view of bench with a ramp (R), checkpoints (numbered blocks), sub-roads (straight) and super-roads (curved).

2.2.7 Complexity

The size of the models required to optimize the design of ramps, while ensuring feasible equipment access to every scheduled mining block grows quickly with the size of the block model. If the complexity of the model is inspected on a per bench basis, then on a bench with N blocks, there are $N \cdot (N-1)$ possible ordered block pairings, each required to be connected by a set of intra-bench roads R_S. Meaning that on a per bench basis the number of binary decision variables required to model accessibility can be roughly described by $N \cdot (N-1) * \overline{|R_S|}$, where $\overline{|R_S|}$ is the average size of the intra-bench road sets. This complexity is problematic as both the number and size of the road sets R_S grows exponentially quickly with the size of the bench.

To solve the related SIP, the proposed method employs an iterative solution procedure, presented in Figure 2-10. The iterative solution procedure splits the entire problem into two components: a ramp configuration component, and a scheduling component. First, an incumbent ramp and road configuration are generated, containing only a small subset of ramps and roads that are to be included in the SIP, limiting the number of binary decision variables and constraints required to model accessibility. The SIP is then optimized using CPLEX, and the algorithm continues by perturbing the incumbent set of ramps and roads, reoptimizing and accepting/rejecting the perturbation using the simulated annealing acceptance criteria (Kirkpatrick et al., 1983).

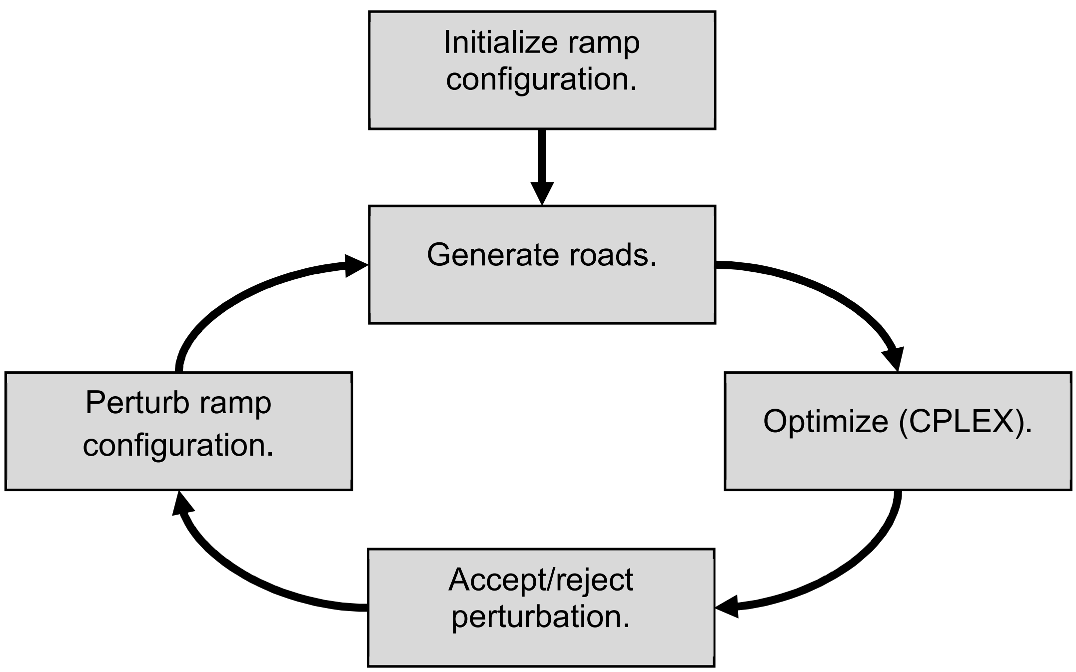

Figure 2-10: Optimization loop.

2.3 Case Study

The method described above is applied to a gold deposit, consisting of a single mine and processor. The mine's block-model contained 10, 500 blocks (10m x 10m x 10m), with gold grade uncertainty described by 10 equiprobable geostatistical simulations, generated via high-order simulation (Minniakhmetov et al., 2018), shown in Figure 2-11. The deposit was scheduled over a period of 7 years, with a mining capacity of 15 Mta, and a processing capacity of 6 Mta.

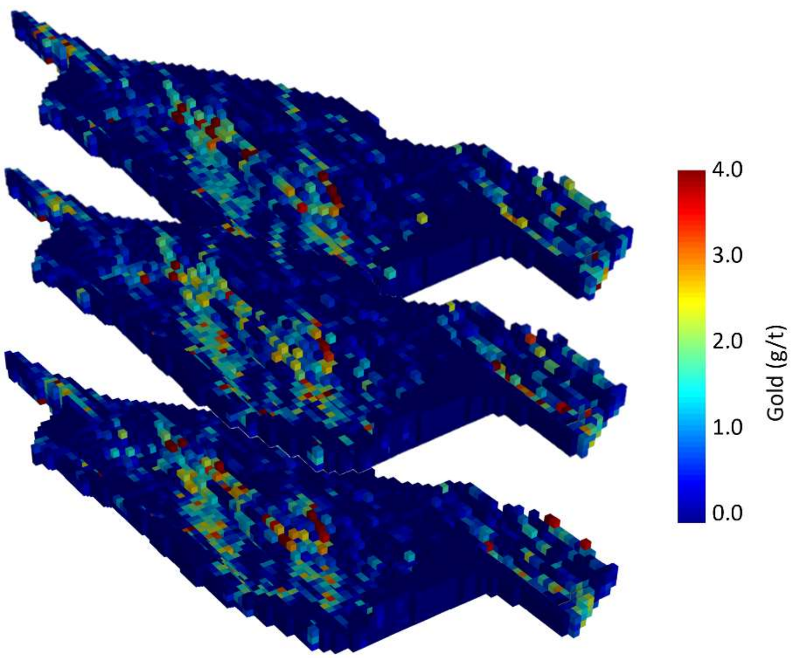

Figure 2-11: Simulated gold grades.

Pre-processing of the block model resulted in the construction of 357 checkpoints, 1942 sub-roads, and 2640 super-roads. The ramps were required to have a width of two blocks, and a centerline length of 3 blocks. The optimization parameters are summarized in Table 2-5.

Table 2-5: Optimization parameters

Parameter	Value
Metal Price ($/oz)	1200
Recovery (%)	90%
Mining cost ($/t)	5
Processing cost ($/t)	15
Ramp placement/removal cost ($)	300,000

Cross sections of the schedule are provided in Figure 2-12 and Figure 2-13, and snapshots of the scheduled blocks and placed ramps for periods 2, 4, and 7 are provided in Figure 2-14. Initially, all mining activity in year 2 and earlier is largely focused on the left side of the pit, providing space for ramp placement, and allowing early access to ore deeper in the mine. As the mine life progresses much of the mining activity migrates to the right wall, where it is uniformly mined until the last period when ore in the bottom of the pit cleaned up.

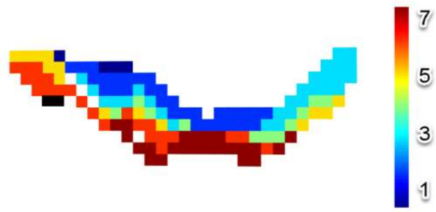

Figure 2-12: Cross-section at x = 39

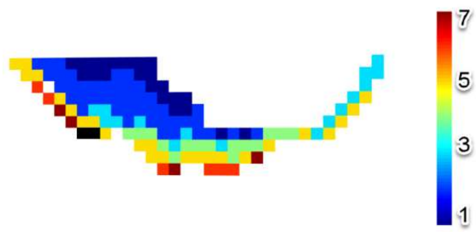

Figure 2-13: Cross-section at x = 52

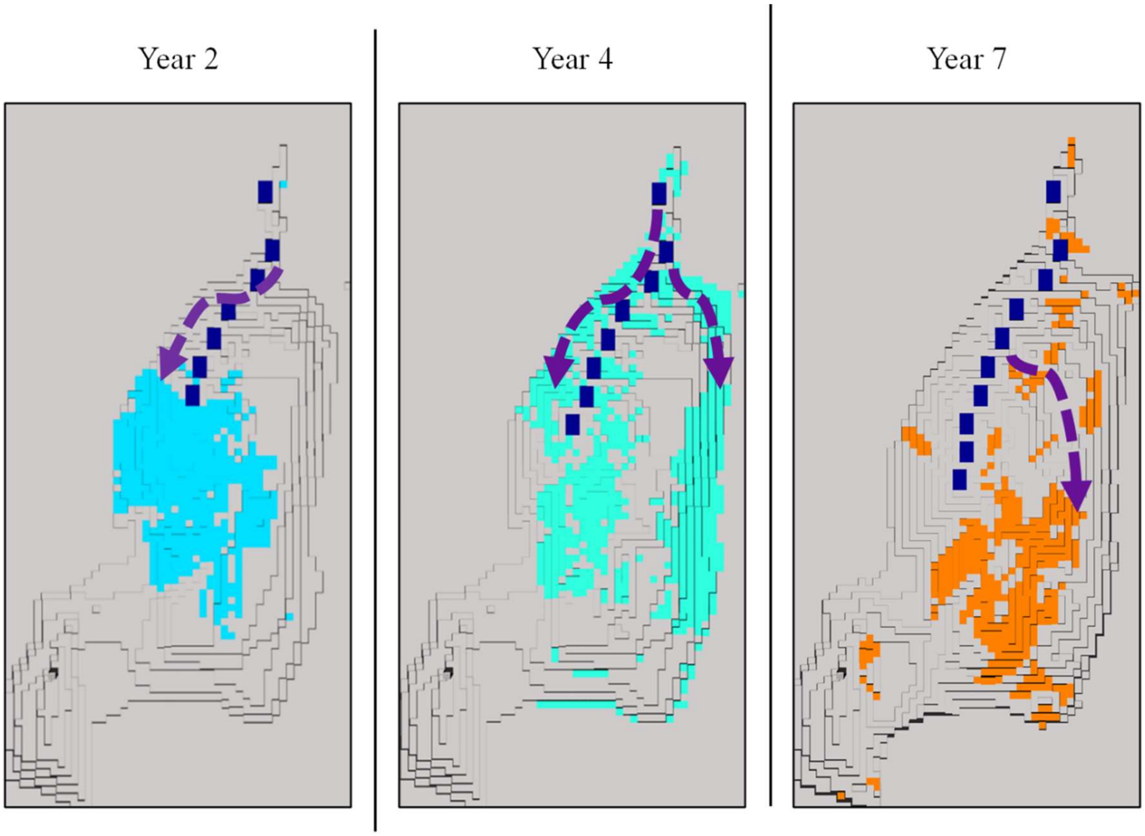

Figure 2-14: Plan view of the open pit denoting mined blocks (light colors) and ramps (dark blue) in years 2, 4, and 7.

A plan view of the final ramp placement can be found in Figure 2-15 and shows that the ramp is placed against the left pit wall. Though several of the ramp segments could be pushed a few blocks tighter to the wall, the overall shape of the ramp closely follows the contour of the pit from crest to the floor. The left side of the pit is also significantly steeper than the right side of the pit, which may result from the blocks on the left side of the pit being closer to the ramp, requiring shorter access roads. Blocks on the right side of the pit are significantly further from the ramp, requiring longer roads, which are much easier than their shorter counterparts to invalidate. As a result, the blocks on the right side of the pit are much harder to access, and the optimizer may have been forced to leave unmined regions to ensure the scheduled blocks can be accessed through the provided roads.

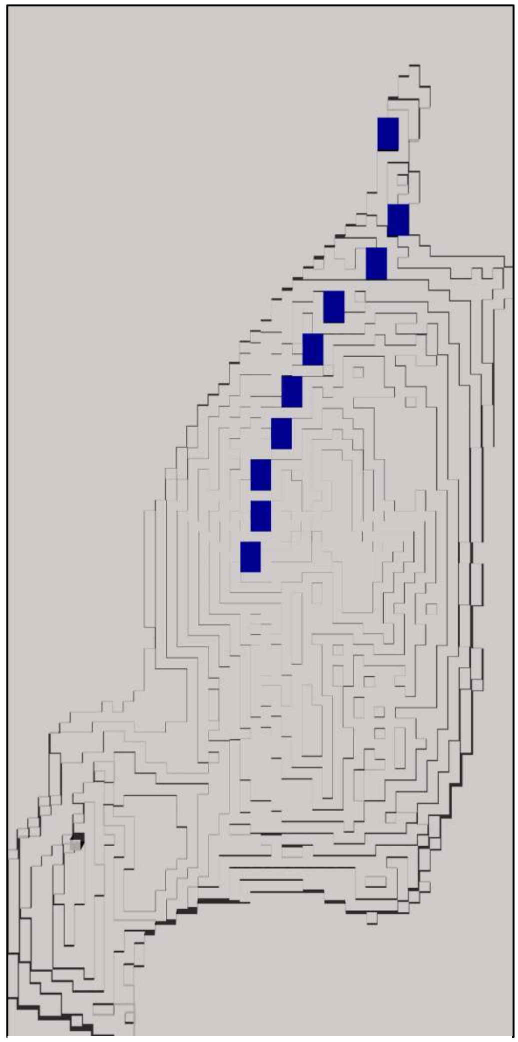

Figure 2-15: Plan view of the open pit denoting final ramp placement (dark blue).

The schedule was forced to dig deep early to meet production targets, resulting in the placement of seven ramp segments in the first period, with only 3 ramp segments placed throughout the remainder of the schedule. The ramp placement profile over the life of mine, along with the cumulative ramp construction cost is provided in Figure 2-16. In total, ramp construction costs \$2.8 million over the life of mine, however, this does not include the additional cost of stripping the required over burden to place the ramps.

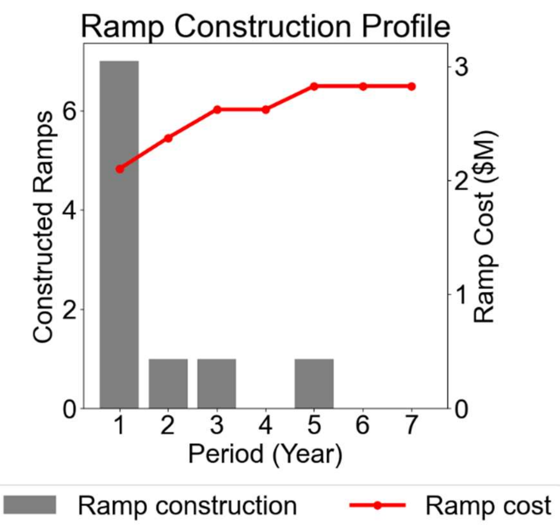

Figure 2-16: Ramp placement profile and cumulative construction costs of optimized ramp design.

Though the SIP had the option to place multiple ramps on the same bench or remove previously placed ramps it chose too never do so. Instead, the optimizer only placed one ramp per bench and left them untouched for the duration of the mine life. The singular ramp per bench strategy likely results from two causes: the ramp configuration provided poor quality options for additional ramps, or the schedule is unable to utilize the benefit provided by an additional ramp. In the first case, the additional ramp options may not provide earlier or more access to ore, meaning the optimizer only incurs the construction cost if the ramp is placed. In the second case, though the ramp may provide earlier or more access to ore, the schedule may be able to saturate production with high grade material using only one ramp, making the additional ramp redundant.

The cumulative discounted cashflow, including ramp construction cost is provided in Figure 2-17. Over the life-of-mine the schedule and ramp design achieve an NPV of $1.1 billion. Though the direct construction cost of the ramps is low, the total effect of ramps on the cashflow is significant as ramps control material availability, impacting when and where mining can happen in the pit. Ramps also require additional stripping of waste material, which incurs a cost, but also consumes production capacity which may otherwise be used for ore.

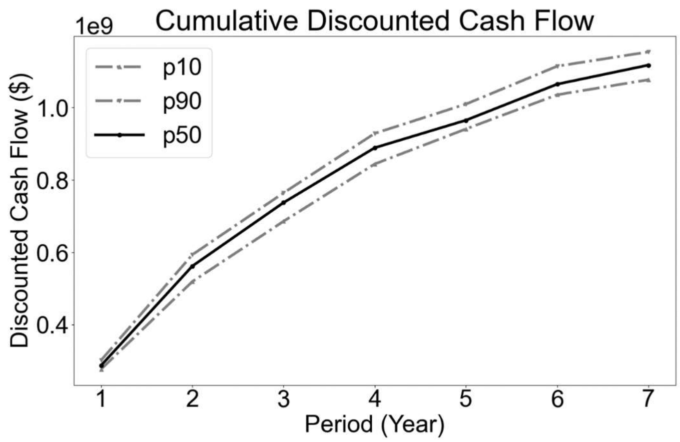

Figure 2-17: Forecasted cumulative discounted cash flow of production schedule and ramp design.

The gold production and average head grade over the life of mine is provided in Figure 2-18. Excluding year 2, where the schedule is likely to exceed the target grade ceiling, the head grade is maintained within its target range of 1.25g/t - 1.5g/t. The corresponding gold production profile mimics the shape of head grade profile, with a peak production of 9 million grams in year 2, and 7-8 million grams in all other years. In the final year, even though the head grade is at its lowest, gold production is maintained relatively high due to the ore tonnage.

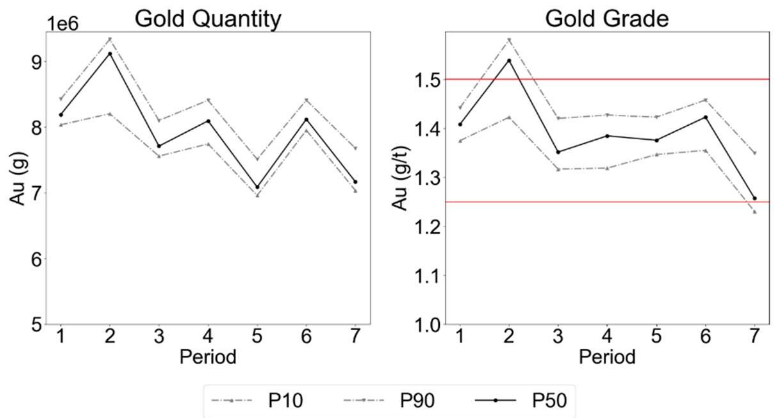

Figure 2-18: Forecasted gold quantity and grade of life-of-mine production schedule.

Figure 2-19 provides the ore tonnage and total tonnage profiles over the life-of-mine. Except for year 5, where a dop in production is observed, the ore production is maintained near the 6 Mta capacity limit. The corresponding total tonnage profile over the life of mine exhibit's large variations in production. In years 1,2,3, and 5 production is at or near the 15 Mta limit, while in years 4, 6, and 7 production decreases to 11, 12, and 11 Mta respectively.

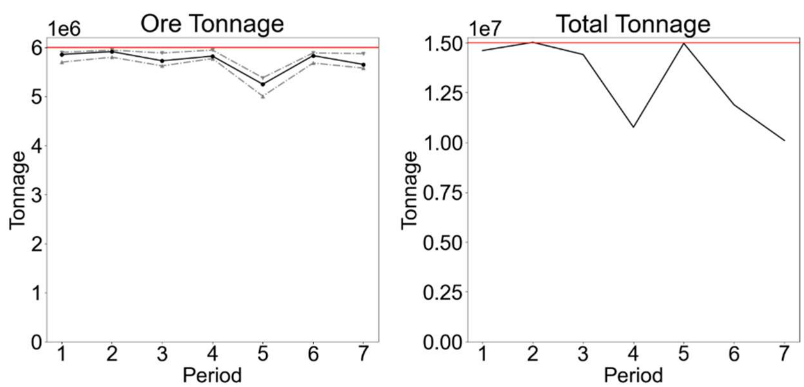

Figure 2-19: Forecasted ore and total tonnages of production schedule.

2.4 Conclusions

An extension to the two-stage SIP proposed in Ramazan and Dimitrakopoulos (2013) for jointly optimizing long-term open pit mine production schedules and ramp design while ensuring feasible equipment access was proposed. The method maximizes the NPV of the production schedule and ramp design while ensuring feasible equipment access to scheduled mining blocks and managing risk of not meeting production targets. The method requires a library of ramps and roads to be predefined, which can be automatically generated by the DFS algorithm presented. From the pre-defined library of ramps and roads, an optimal ramp design and schedule is generated, while ensuring equipment access through the selected ramps and provided roads.

The method was applied to a gold deposit, with gold grade represented by 10 geostatistical simulations, to develop a life of mine production schedule and ramp design. The optimized ramp design closely followed the contour of the pit on the left side and the associated optimized production schedule maintained gold grade within the target range, while satisfying processing and mining capacities. The results demonstrate the methods ability to jointly optimize the ramp design and schedule, producing a ramp design that provides access to desirable material in each period and an optimized schedule that utilizes the material access provided by the ramp.

The joint stochastic optimization of long-term open pit mine production schedules and ramp design extends the formulation proposed in Ramazan and Dimitrakopoulos (2013). Future research in this direction should seek to incorporate this method into the simultaneous optimization of mining complexes (Dimitrakopoulos and Lamghari, 2022). Additionally, the method only considers the construction cost of the ramps and not the associated haulage costs. Extending the method to incorporate haulage costs would enable better haul road design.

Chapter 3. Optimizing Multi-element Cut-off Grades for a Strategic Production Plan Under Geological Uncertainty

3.1 Introduction

Conventionally, mine planning is conducted in several sequential steps, with each successive step relying upon the previous. The process starts with cut-off grade optimization, which is traditionally optimized through Lane's method (Lane, 1964), providing the optimal cut-off grades in each year over the life-of-mine to maximize net present value (NPV) considering a global deterministic distribution of material. However, mines operate in uncertain heterogenous environments, which, in combination with the long-term schedule, significantly influence the quantity and quality of material available each year. Additionally, the sequential process of the conventional approach leads to sub-optimal strategic plans, as the cut-off grade, production schedule, and other components of a mining complex are interdependent. Here, a method for optimizing long-term multi-element cut-off grades for an optimal production plan under geological uncertainty is proposed, addressing the issues inherent in the traditional stepwise sequential process.

Lane's theory provides the optimal cut-off grade policy over the life of the mine, defining the optimal cut-off grades in each year to maximize NPV (Lane, 1964; 1988; Rendu, 2014). Lane's method considers the grade tonnage curves based upon deterministic estimate of the deposit (David, 1977; Journel and Huijbregts, 1978), fixed costs, and the concept of an opportunity cost to solve for the optimum cut-off grade in each year over the life of the mine. The opportunity cost is the penalty incurred for not receiving future cash flows earlier due to the cut-off grade decision taken now. Though, typically used for single elements, Lane's method can be extended to multiple elements by including the contribution of both elements in the cashflow, enabling computation of the optimal cut-off grade for each element. However, Lane's method does not consider the production schedule, which defines the quantity and quality of material mined each year, as a result, the global grade-tonnage curves which Lane's method relies upon are not representative of the material available in each period, and it is difficult to extend Lane's method to consider geological uncertainty.

Asad and Dimitrakopoulos (2013) provide an extension of Lane's method which considers geological uncertainty and defines a single-element cut-off grade policy suitable for single mine operations with multiple processing stream destinations. Geological uncertainty is represented by a set of geostatistical simulations, modeling the uncertainty and variability of grades in space (Goovaerts, 1997). Accounting for geological uncertainty when optimizing cut-off grades allows risk to be managed and increases value as mined material is subjected to non-linear transfer functions and as it is transformed from a raw material into a sellable product. However, the extension is limited to non-stockpiling destinations. Nonetheless, the method demonstrates the importance of incorporating the geological uncertainty into the determination of cut-of grades.

Menabde et al. (2018) provides a stochastic integer programming formulation for jointly optimizing open pit mine production schedules and cut-off grades for a single element under geological uncertainty. In this formulation the standard extraction decision variable x_{it} (decision to extract block i in year t) is extended to x_{ijt}, representing the decision to extract block i under cut-off grade j in year t. This approach requires discretizing the range of possible cut-off grades into a finite set of predefined cut-off grades, and the optimal cut-off grade is chosen from within that set for each year. As a result of the discretization process, the optimized cut-off grades are approximations of the true optimal cut-off grades in each year and depend on the quality of the discretization. Additionally, the formulation is limited to a single element and two destinations. Nonetheless, this method presents a significant departure from the traditional framework, in that cut-off grades are jointly optimized with the production schedule, making cut-off grades an output of the method, rather than an input.

Asad et al. (2016) present a literature review of cut-off grade optimization. The review covers Lane's method and its extensions to include multiple elements, multiple destinations, and uncertainty from various sources, and mathematical programming methods. The authors note the limitations of Lane's method, which become more problematic for complex mining operations, causing the method to miss optimum cut-off grades, an issue which is largely addressed by mathematical programming methods.

The simultaneous stochastic optimization (SSO) framework optimizes entire mining complexes considering uncertainty from multiple sources under a single mathematical formulation (Montiel and Dimitrakopoulos, 2015; Goodfellow and Dimitrakopoulos, 2016; 2017; Montiel and Dimitrakopoulos, 2017; 2018; Kumar and Dimitrakopoulos, 2019; Dimitrakopoulos and Lamghari, 2022). The SSO framework optimizes production schedules, destination policies, and downstream decision variables. For single elements, the destination policy is defined as a single element cut-off grade policy and optimized similarly to (Menabde et al., 2018), however for multiple elements a block based or cluster based destination policy is employed. Block and cluster-based destination policies used in the SSO framework have a high degree of resolution and can send material in advantageous ways, positively effecting the value of the mining complex.

Block based destination policies are useful tools for optimizing production schedules, however, the are operationally difficult to implement, limiting their usefulness for strategic planning. Block based destination policies assign a destination directly to a mining block and can either be scenario independent or dependent. Scenario independent policies may misclassify material as the properties of the block change from one simulation to the next and may result in waste being sent to the mill or ore being sent to the waste dump. Scenario dependent policies address the issue of material misclassification by enabling blocks to be sent to different destinations in different scenarios, however, they are of little operational use as reality does not perfectly align with the scenarios.

Cluster based destination policies function differently, in that they can assign destinations to regions in grade space, rather than directly to blocks. Clusters may be constructed from k-nearest-neighbor (KNN) (Fix and Hodges, 1989), which assigns blocks to clusters based on the nearest centroid. Since the grades of a block change from one simulation to the next, the destination of that block can also change as the nearest centroid depends on the grade values in each simulation, addressing the issue of misclassification. Similarly, any point in grade space can be classified based on the nearest centroid, allowing unseen blocks of any grade to be classified. The ability of cluster-based destination policies to classify unseen blocks makes them technically amenable to operational use. However, their complexity and lack of interpretability make them difficult to use. For presentation purposes, an example of a cluster-based destination policy is shown in Figure 3-1, which, though simplified, still demonstrates the complexity of such a destination policy, as the boundary between destination regions is complex, and non-linear.

Though such destination policies are advantageous in that they are simultaneously defined with the production schedule and are thus optimal for the spatial distribution of grades, production plan, and configuration of the mining complex. They are not directly translatable to cut-off grades, which, are required to define where to send material upon extraction in an operating environment. Additionally, previously discussed methods for directly defining cut-off grades are to computationally expensive to be effectively employed in the SSO framework.

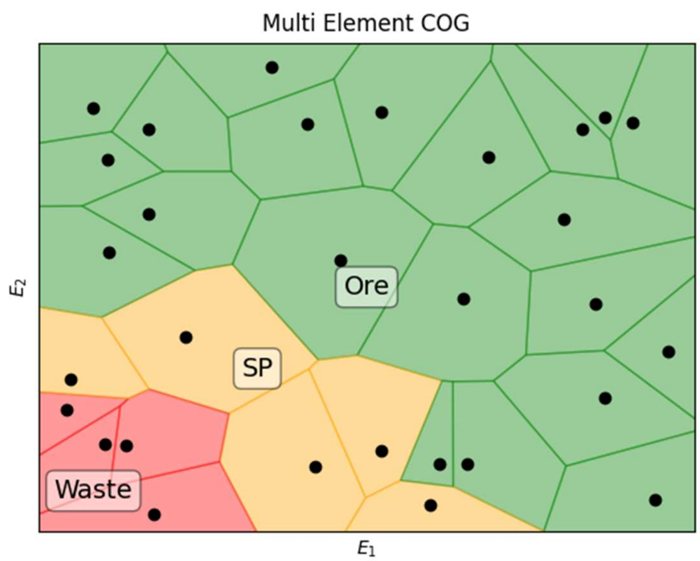

Figure 3-1: Cluster based destination policy

This work proposes two multi-element cut-off grade definitions, and a method for optimizing multi-element cut-off grades under geological uncertainty considering an optimal production plan. The method is similar to (Menabde et al., 2018), in that the cut-off grades are optimized considering the long-term schedule, however, the proposed method is suitable for multiple elements and destinations. The cut-off grades are optimized using reinforcement learning (Sutton and Barto, 2018) to minimize deviations from long-term mine plan forecasts. In the following sections the method is presented, followed by an application on a gold and copper mine with conclusion following.

3.2 Method

3.2.1 Formulation

To optimize multi-element cut-off grades for an optimal production schedule to minimize deviations from long term mine plan forecasts (e.g. metal production, mill tonnage, stockpile tonnage, etc.), the proposed stochastic mathematical program minimizes the deviation d for each property $p \in P$, in each year $t \in T$ for each geological scenario $s \in S$. The deviation $d_{p,s,t}$ is formulated as the absolute difference between the target forecast value $\bar{F}_{p,s,t}$ and the forecasted value under the cut-off grade policy $F_{p,s,t}$.

$$minimize \frac{1}{|S|} \sum_{s \in S} \sum_{t \in T} \sum_{p \in P} d_{p,s,t} \quad (13)$$

$$d_{p,s,t} \geq F_{p,s,t} - \bar{F}_{p,s,t} \forall p \in P, \forall s \in S, \forall t \in T \quad (14)$$

$$d_{p,s,t} \geq \bar{F}_{p,s,t} - F_{p,s,t} \forall p \in P, \forall s \in S, \forall t \in T \quad (15)$$

The target forecast value $\bar{F}_{p,s,t}$ is required as input, but $F_{p,s,t}$ is computed as a function of the cut-off grades in the current period and the current state of the mining complex. For each year t and scenario s, $F_{p,s,t}$ can be computed as follows, where f denotes a function, cog_t is cut-off grade policy for period t, defining the threshold values for all elements, and $\mathcal{s}_{s,t}$ is the state of the mining complex in scenario s in period t. The state contains relevant information about the mining complex for each scenario in each period, such as grade-tonnage curves, and stockpile properties per scenario.

$$F_{p,s,t} = f_p(cog_t, \mathcal{s}_{s,t}) \forall p \in P, s \in S, t \in T \quad (16)$$

The state $\mathcal{s}_{s,t}$ is dependent on the previous state $\mathcal{s}_{s,t-1}$ and the cut-off grade policy cog_t, allowing formulating the problem as a Markov decision process (MDP) (Howard, 1960). The state space $\mathbb{S}$ of the MDP is continuous, containing information about the mining complex in each period, such as the grade-tonnage curves, and stockpile properties. The action space $\mathbb{A}$ is continuous and contains all parameters to define cut-off grades, with each action $\boldsymbol{a}$ being a vector in $\mathbb{R}^n$, where n is the number of parameters required to define cut-off grade.

$$\boldsymbol{a} = (a_1, \dots, a_n) \quad (17)$$

The reward for taking action a in state s and transitioning to state s' is computed per equation 18, where w_p is a weight applied to each property and $d_{p,s'}$ is the deviation from forecast from property p in state s', and is computed similarly to above.

$$R_a(s, s') = \sum_{p \in P} w_p d_{p,s'} \tag{18}$$

Transitioning from state s to s' is performed by sending material flow through the mining complex according to the cut-off grade policy defined by action a. Some components of the state representing the mining complex do not depend on the previous state, such as grade tonnage curves, as the action a taken in state s does not affect the grade tonnage curve in state s'. However, other components, such as stockpiles, which retain material across periods, depend on the previous state s and action a. The transition from state s to s' after taking action a is defined by the transition function.

$$s' = T(s, a) \tag{19}$$

Minimizing the sum of rewards received over the length of an episode aligns with the goal of minimizing deviations from forecasts over the life of mine and requires optimizing a policy π for action selection in each state. An optimal policy π^* is defined as follows.

$$\pi^*(s) = \arg\min_a \left(R(s, a) + \gamma \sum_{s'} p(s, a, s') V(s') \right) \tag{20}$$

To find the optimal policy minimizing deviations from target forecasts, Proximal Policy Optimization (PPO) (Schulman et al., 2017), a reinforcement learning algorithm, is employed, as it is suitable for continuous action and state spaces. PPO tries to take large steps, without collapsing the solution. Generally, there are two main variations of the algorithm, PPO-Penalty, which penalizes large changes in the policy, and PPO-Clip which clips large changes in the policy. Here, PPO-Clip is used.

3.2.2 Cut-off Grade Policies

Cut-off grade policies define decision boundaries delineating the space of grades. To minimize deviations from forecasts (Eq. 1) the cut-off grade policy must consider the combined contribution of all elements and the decision boundary must be defined as a function of all elements. Here, two multi-element cut-off grade policies are proposed; termed the orthogonal and diagonal cut-off grade policies, which may be applied to any number of elements and destinations.

3.2.2.1 Orthogonal Cut-Off Grade Policy

The orthogonal multi-element cut-off grade policy is a natural extension of the single element cut-off grade policy. Threshold values are defined for each element, functioning as orthogonal decision boundaries, dividing the space of all possible grades into two or more regions. Each region is assigned a destination, and any material with grade values corresponding to a point within that region is sent to that destination. For the 2-element example provided in Figure 3-2, the action vector (Eq. 4) would be defined in $\mathbb{R}^4$ as $(E_{1_{low}}, E_{2_{high}}, E_{2_{low}}, E_{2_{high}})$, having two cut-off grades for each element, dividing the space of all possible grades into nine rectangular regions. Though the example is formulated for two economic minerals, handling deleterious elements is trivial and can be achieved by assigning regions with greater quantities of deleterious elements as waste or stockpile. More elements can be considered with this cut-off grade policy by adding more dimensions. The size of the regions is controlled by increasing or decreasing the low and high cut-off values for each element Each threshold value corresponds to an entry in the action vector, and each year, the agent acts by selecting these cut-off values and receives a reward as described above. Additionally, the corresponding destination for each region can also be controlled, allowing for fine control over where material is sent upon extraction. However, the orthogonal policy poorly captures the combined contribution of elements towards the decision of where to send material upon extraction. For example, consider a block with a grade slightly below the low cut-off for element 1 and 2 in the example provided. Under this policy, that block would be sent as waste. However, it is likely that the combined contribution of both elements (assuming they are both economic) would make the block worth stockpiling.

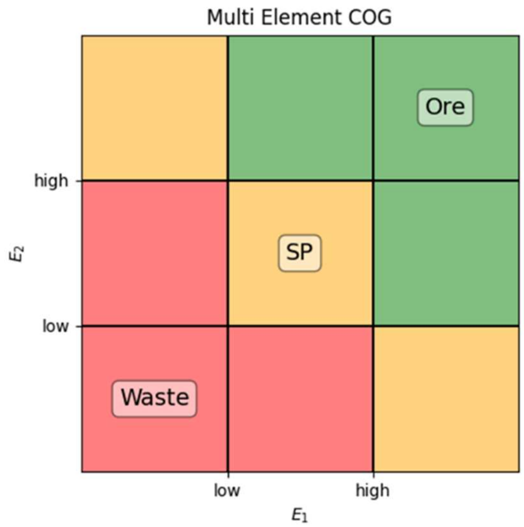

Figure 3-2: Orthogonal cut-off grade policy for two elements and three destinations.

3.2.2.2 Diagonal Cut-Off Grade Policy

Like before, threshold values are defined for each element, however, each element is required to have the same number of threshold values. Each of the thresholds defines the intersection points of the decision boundary. In the two-element example in Figure 3-3, two thresholds are defined for each element, dividing the space into three regions. The decision boundary between the waste and stockpile material is defined by the low threshold for each element, and the decision boundary between the stockpile and mill material is defined by the high threshold for each element. Deleterious elements can be handled by this policy, in the provided two-element example, the slope of the lines simply need to be positive. Like the Orthogonal cut-off grade policy, more elements may be included by adding more dimensions. For example, the diagonal policy could be defined for three elements, with each threshold defining a surface in the three-dimensional grade space. Like the Orthogonal policy, each threshold corresponds to an entry in the cog_t vector, and each year the agent acts by selecting the high and low threshold values for each element and receives a reward corresponding to the deviations from forecast. Though the diagonal method has fewer regions than the orthogonal policy, the size and shape of the regions are controllable, enabling fine control over how to send material upon extraction from the mine. Additionally, since the decision boundaries are non-orthogonal, they may be better able to capture the combined contribution of multiple elements.

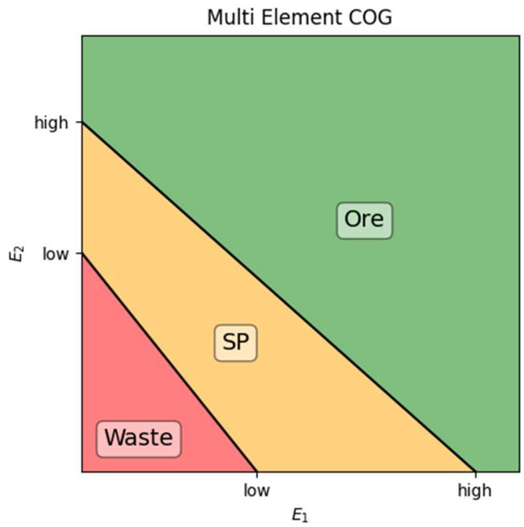

Figure 3-3: Diagonal cut-off grade policy for two elements and three destinations

3.3 Case Study

The mining complex, shown in Figure 3-4 used for testing the multi-element cut-off grade policies is composed of a mine, which can send material to a waste dump, stockpile, or mill. The mine has two economic minerals, gold and copper, with grade uncertainty and variability represented by 15 simulations obtained with direct block simulation of multiple correlated attributes (Boucher and Dimitrakopoulos, 2009). The entire mining complex was simultaneously optimized using the SSO framework (Goodfellow, 2014), providing an optimized production schedule, destination policy, and downstream decisions.

Both previously presented multi-element cut-off grade policies are tested, and their performance compared. The policies are optimized to minimize deviations from the SSO forecasts that were generated with the cluster-based destination policy.

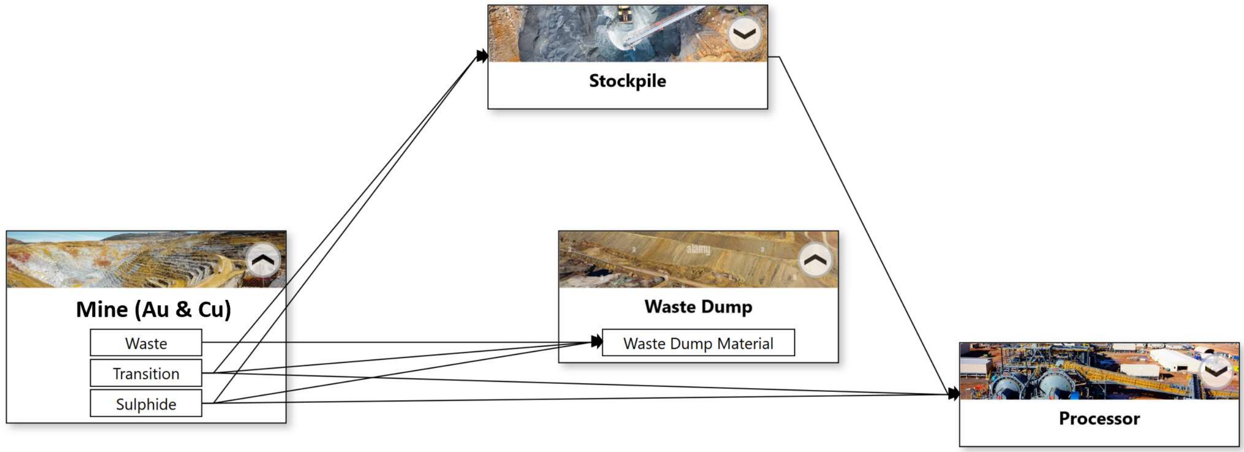

Figure 3-4: Gold and copper mining complex

The reward (Equation 4) was constructed such that deviations in mill and stockpile tonnage, and deficits in mill metal were penalized. The mill tonnage and metal were deemed to be the most important forecasts, and thus weighed greater in the reward. Only metal deficits were penalized, rather than deviations because it was difficult to reproduce the exact forecasted quantities for both metals, usually resulting in one metal being below forecast. Penalizing only deficits improved performance in this regard as the agent was more likely to develop multi-element cut-off grade policies that met or exceeded both metal forecasts.

The state space was formulated as defined in Section 3.2, with grade-tonnage curves for each element in each scenario, and the stockpile properties in each scenario. The grade-tonnage curves in each period are independent of the cut-off grade policy, thus can simply be computed from the scheduled blocks. However, the stockpile retains material across periods, thus, depends on the stockpile properties in the previous period, the cut-off grades, and the grade-tonnage curves.

3.3.1 Orthogonal Multi-Element Cut-Off Grade Policy

The forecasted gold quantities for both the SSO (denoted as SSO), and the orthogonal cut-off grade policy (denoted as COG) are shown in Figure 3-5. The orthogonal multi-element cut-off grade policy reproduces reasonably well the SSO gold forecast achieved using the cluster-based destination policy. The P50 line matches best in the first five years, but trends slightly downward away from the SSO forecasts towards the end of the mine life. The P10 line is also reproduced well by the multi-element cut-off grade policy, but the P90 line of the multi-element cut-off grade policy falls below that of the original SSO forecast.

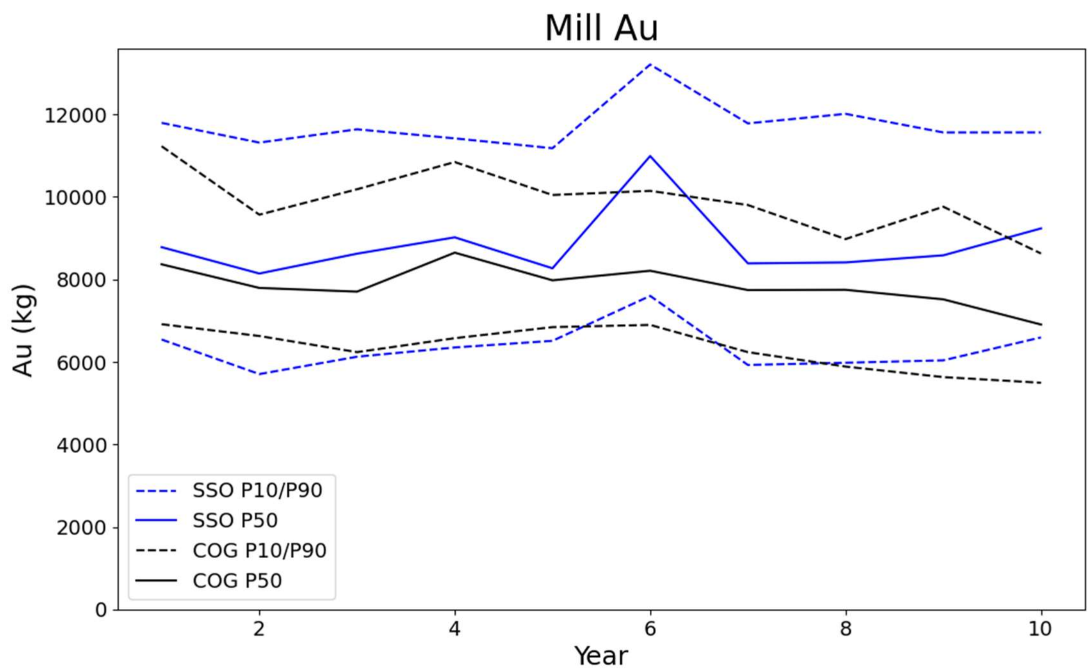

Figure 3-5: Orthogonal cut-off grade policy vs SSO mill gold forecast

The copper forecasts are also well reproduced as shown in Figure 3-6. Like with the gold forecasts, the copper forecasts are reproduced best in the first few years, but trend slightly downward away from the SSO forecasts toward the end of the mine-life. However, in contrast to the gold forecasts, the P90 lines are similar for the orthogonal cut-off grade policy and the SSO forecasts, but the P10 differ. The orthogonal multi-element cut-off grade policy has a much higher P10 line compared to the SSO forecast.

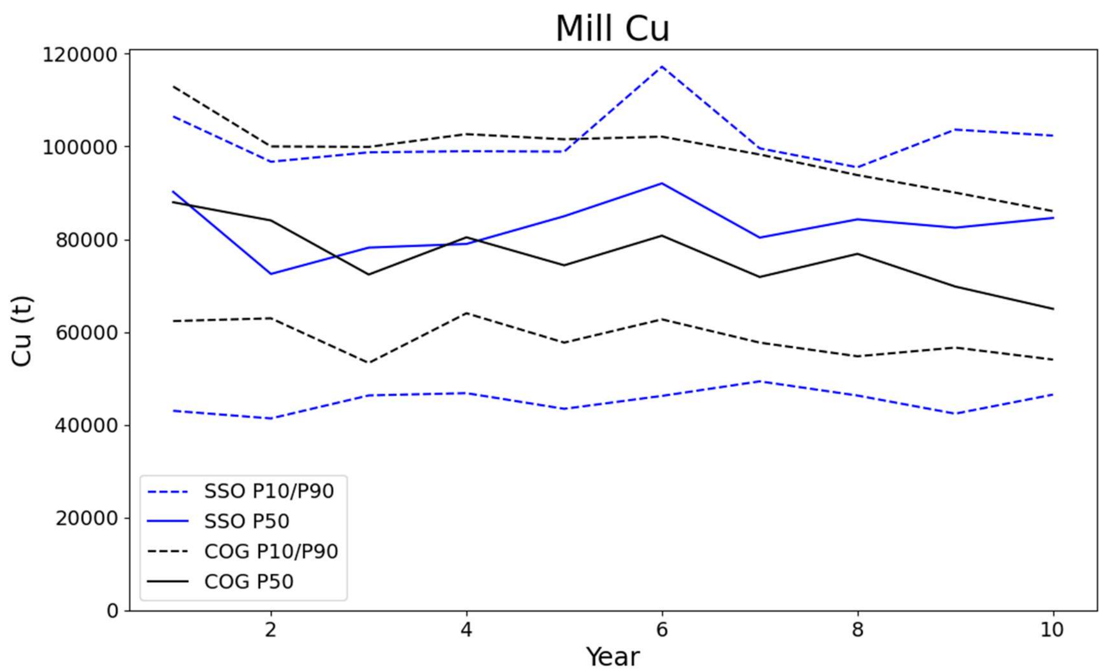

Figure 3-6: Orthogonal cut-off grade policy vs SSO mill copper forecast

The mill tonnage forecasts are shown in Figure 3-7. The mill tonnage forecast for orthogonal cut-off grade policy is similar to the mill tonnage SSO forecast. The P90 forecast of the orthogonal cut-off grade policy is higher than the P90 SSO forecast and exceeds the 30 mt mill capacity. The high P90 results from the method trying to satisfy the metal forecasts. In all years at least one of the metal forecasts is low, thus encouraging the agent to send more material to the mill.

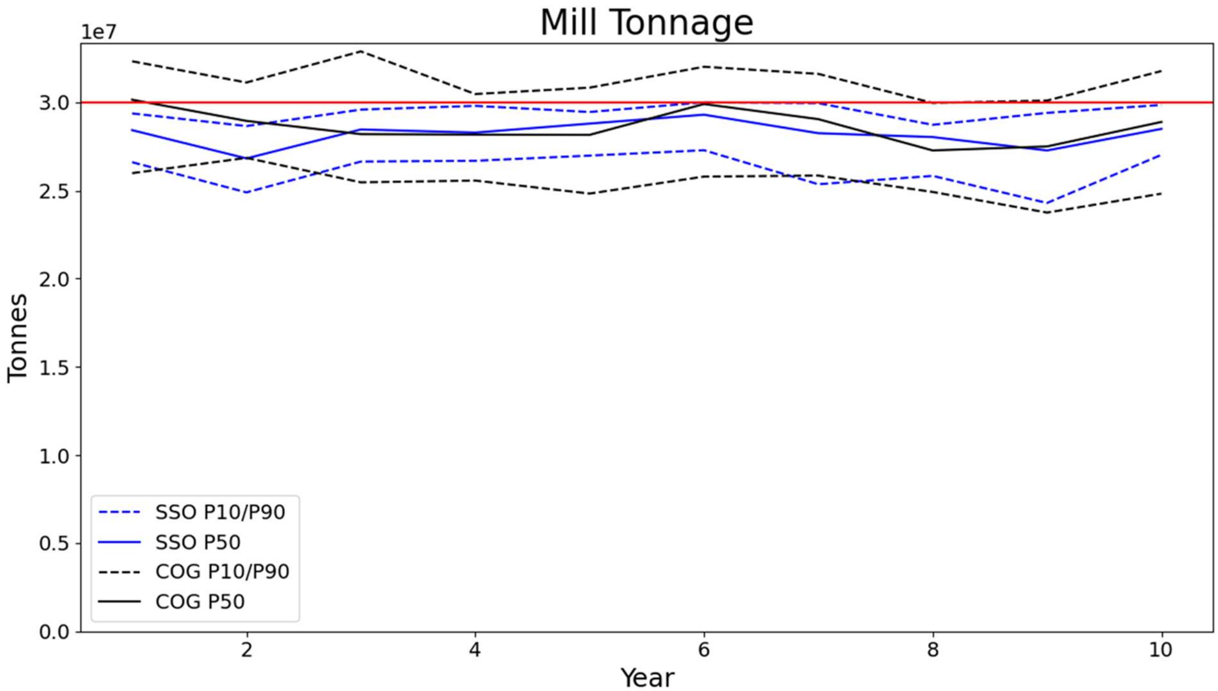

Figure 3-7: Orthogonal cut-off grade policy vs SSO mill tonnage forecast

The stockpile tonnage forecasts for the orthogonal cut-off grade policy and SSO are provided in Figure 3-8. The deviation weights for the stockpile tonnage were low compared to the mill metal and tonnage deviation weights, thus exact reproduction of the stockpile tonnage forecast was not expected. However, the two forecasts have similar shapes, with a peak towards the beginning and another towards the end of the mine life. To better reproduce the SSO stockpile forecasts, the weight for stockpile deviations could be increased, however, this would likely deteriorate reproduction of other forecasts, or the additional cut-off grades could be added to increase the resolution of the policy.

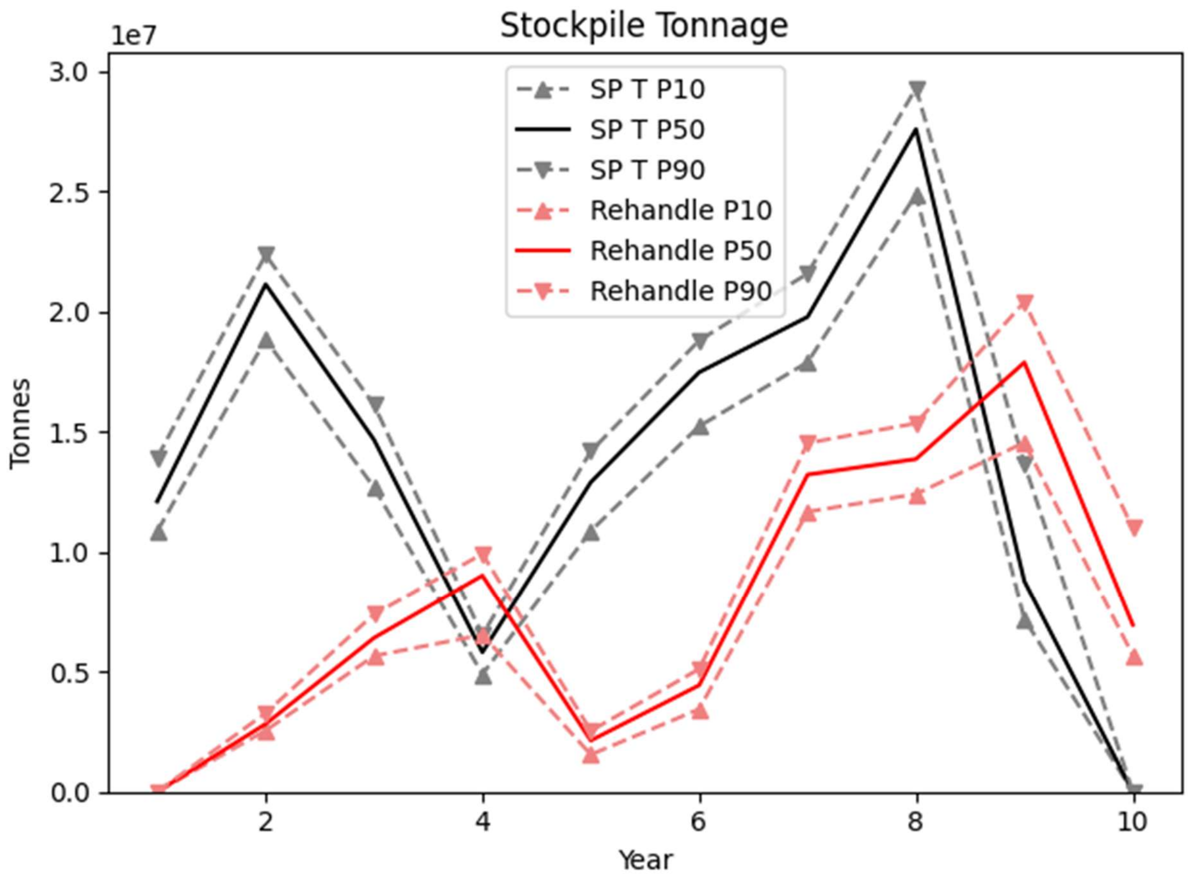

Figure 3-8: Orthogonal cut-off grade policy vs SSO stockpile tonnage forecast

The NPV of the orthogonal policy is notably lower than the original SSO forecasts, with a P50 of \$1.5B compared to \$1.9B. The lower NPV of the orthogonal policy results from the lower Au production at similar mine tonnages. The Risk profile of the NPV for the orthogonal policy is also wider, with a P10/P90 of \$1.0B/\$2.0B compared to \$1.8B/\$2.1B for the SSO forecasts. The larger risk profile results from the orthogonal policy having lower resolution than the cluster-based destination policy.

3.3.2 Diagonal Multi-Element Cut-Off Grade Policy

The mill tonnage forecast for the diagonal cut-off grade policy is presented in Figure 3-9. The diagonal policy matches the SSO forecasts for the duration of the mine life, with the exception of year 6, where the cluster-based policy has a significant increase in gold which is not captured in the cut-off grade policy. Compared to the orthogonal cut-off grade policy, the diagonal cut-off grade policy performs much better in terms of reproducing the SSO gold forecast.

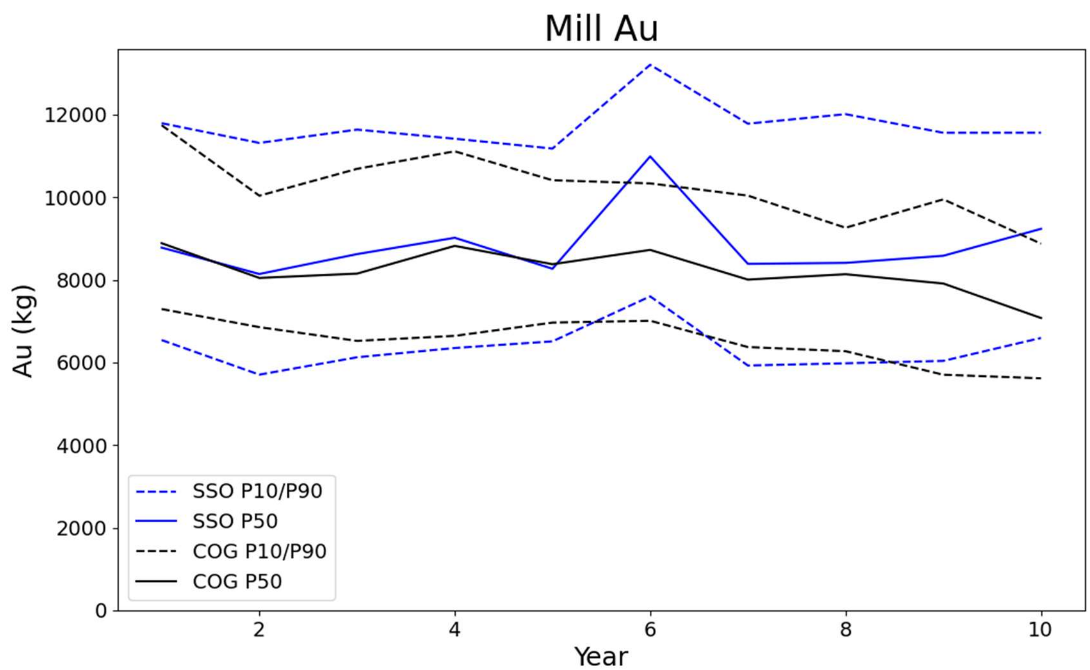

Figure 3-9: Diagonal cut-off grade policy vs SSO gold forecast

The diagonal cut-off grade policy is also able to closely match the copper forecasts, as shown in Figure 3-10. The P50 and P90 lines are similar throughout the mine life, however, the P10 line for the diagonal cut-off grade policy is higher than the P10 line for the SSO forecast. Compared to the orthogonal cut-off grade policy, the diagonal cut-off grade policy better reproduces the SSO copper forecasts.

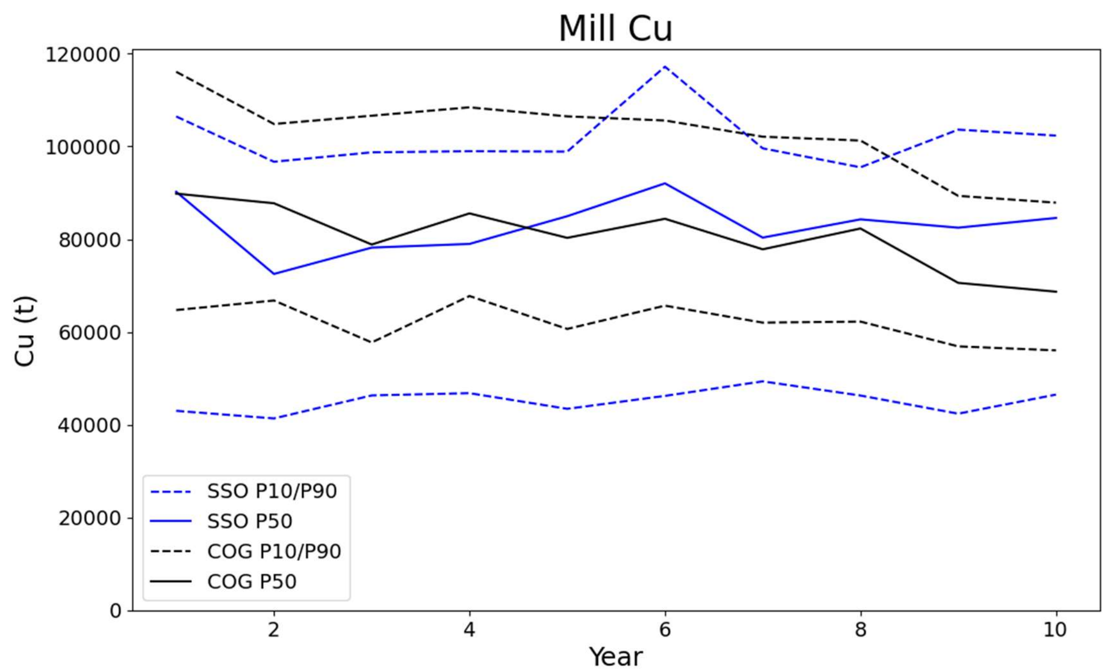

Figure 3-10: Diagonal cut-off grade policy vs SSO copper forecast

The mill tonnage forecasts for the diagonal cut-off grade policy are similar to the SSO forecasts, as shown in Figure 3-11. Similarly, to the orthogonal cut-off grade policy, the diagonal cut-off grade policy matches well to the SSO forecasts in terms of the P50, but the P90 line is high. The high P90 line results from the agent trying to satisfy the metal forecasts at the mill, thus encouraging the agent to accept the penalty incurred.

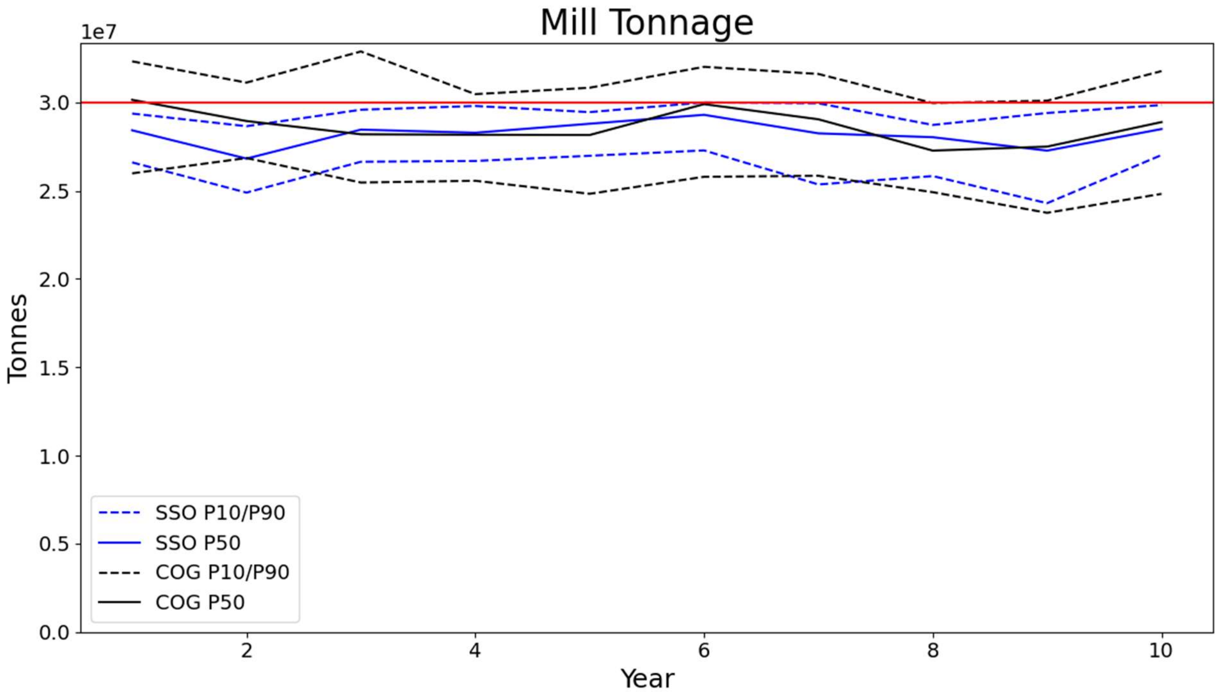

Figure 3-11: Diagonal cut-off grade policy ss SSO policy mill tonnage forecast

The stockpile tonnages for the diagonal cut-off grade policy are provided in Figure 3-12. The deviation penalty cost for the stockpile tonnages was lower than the penalty cost for mill tonnage and metal deviations, thus exact reproduction of the stockpile tonnage forecast was not expected. However, the tonnage profile for the diagonal cut-off grade policy has a similar shape to the SSO forecast, with a peak towards the beginning and the end of the mine life. Additionally, the tonnage profile for the diagonal cut-off grade policy is very similar to the tonnage profile for the orthogonal cut-off grade policy. To better reproduce the SSO stockpile forecasts, the weight for stockpile deviations could be increased, however, this would likely deteriorate reproduction of other forecasts, or the additional cut-off grades could be added to increase the resolution of the policy.

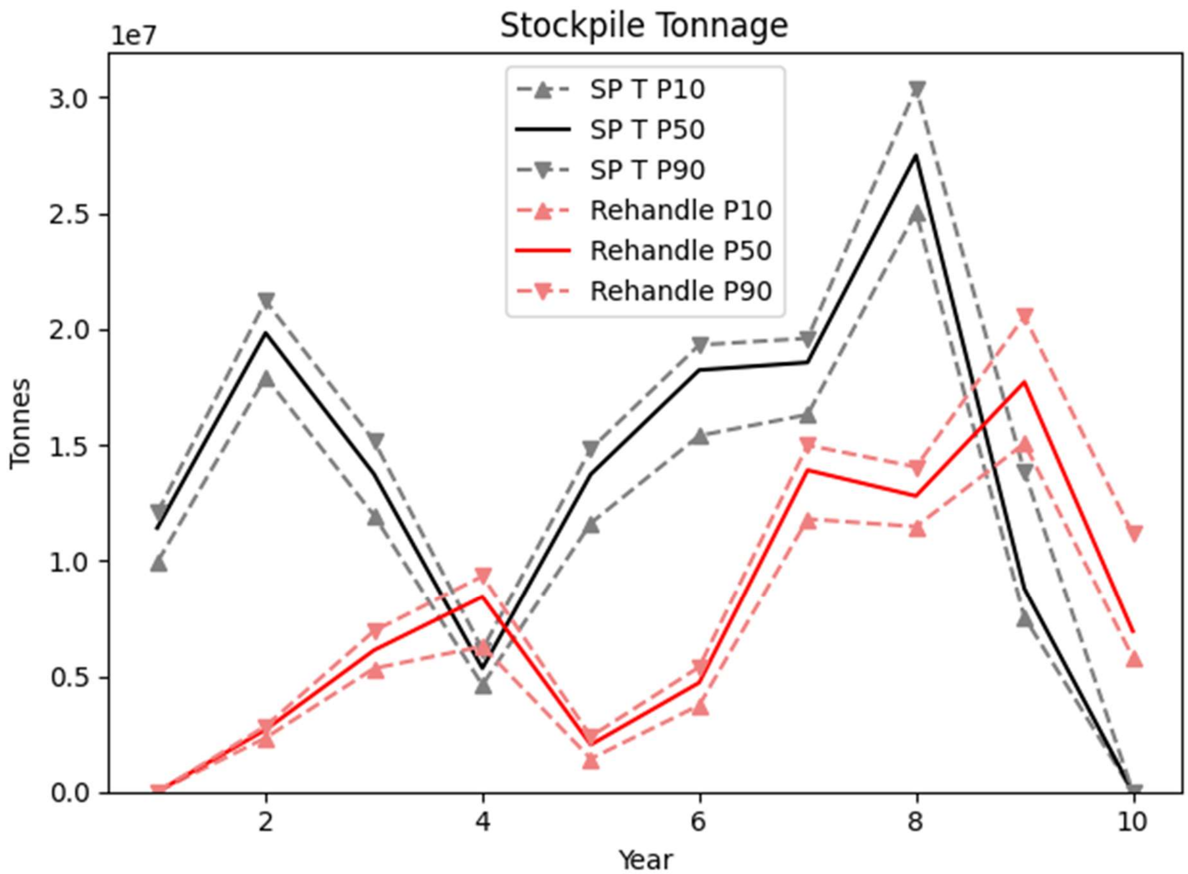

Figure 3-12: Diagonal cut-off grade policy vs SSO stockpile tonnage forecast

The NPV of the diagonal cut-off policy performs similarly to the SSO forecast, with a P50 NPV of $1.8B compared to $1.9B. However, the risk profiles remain wider, with a P10/P90 of $1.3B/$2.0B, compared to $1.8B/$2.1B for the SSO forecasts. The lower NPV of the diagonal policy again result from the lower resolution of the cut-off grade policy compared to the cluster-based SSO forecast.

3.3.3 Cut-off Grades

The optimized cut-off grades are presented Figure 3-13. Notably, the optimal cut-off grades do not follow the standard intuition that cut-off grades are high in early years and decrease over the life of mine. These unintuitive cut-off grades may result from the cut-off grades coming from the schedule; thus, the cut-offs are informed by the spatial distribution of grades and quantity and quality of material available in each year. In early years of production, low quantities of high-grade material may be uncovered, requiring low cut-off grades. However, in later periods, after significant excavation, more high-grade material may be uncovered, allowing higher cut-off grades.

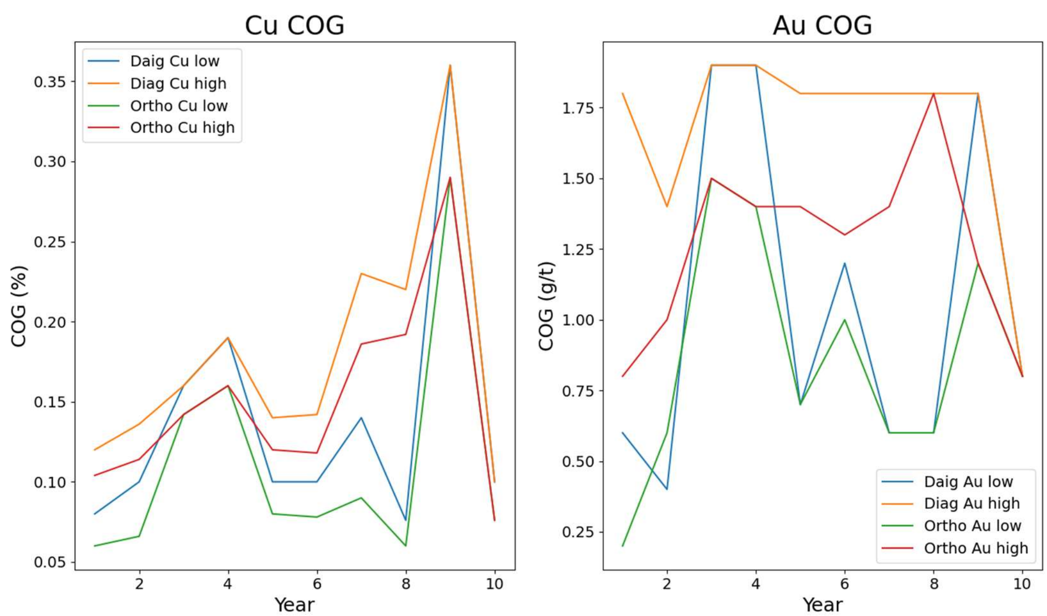

Figure 3-13: Optimized cut-off grades

3.4 Conclusions

A reinforcement learning framework for optimizing multi-element cut-off grades under supply uncertainty given a production schedule is presented and applied to a gold and copper mining complex. The orthogonal multi-element cut-off grade policy defines orthogonal decision boundaries dividing the space of grades into rectangular regions, which, though simple, are unable to capture the combined contribution of multiple elements. The diagonal multi-element cut-off grade policy improves upon the orthogonal cut-off grade policy in this regard, by allowing a linear relationship to be modelled, however, this comes at the cost of increased complexity.

Both proposed multi-element cut-off grades were applied to a gold and copper mining complex composed of a mine, waste dump, stockpile, and mill. The reinforcement learning framework optimized orthogonal and diagonal cut-off grade policies and the performance of the multi—element cut-off grades was assessed. Though both methods were found to perform well, the diagonal multi-element cut-off grade policy performed better than the orthogonal multi-element cut-off grade policy, better reproducing the target forecasts with higher NPV. However, other mining complexes may exist where the orthogonal policy performs better as the performance of each method is highly dependent on the distribution of material. Additional research in the area may also identify superior policies that performs better than both the orthogonal and diagonal policies.

The proposed multi-element cut-off grade policies provide operationally usable multi-element destination policies capable of meeting target forecasts. The diagonal cut-off grade policy was found to perform better than the orthogonal cut-off grade policy on the presented case study. Both methods deviated from the stockpile forecasts as stockpile deviations were not weighed as greatly as mill metal and tonnage deviations. Future research should aim to improve stockpiling performance through different cut-off grade definitions, or by increasing the number of cut-off grades. Additionally, the performance of the method with three or more elements should be tested as additional elements increases the dimensionality of the problem.

Chapter 4. Conclusions

Conventional strategic mine planning is performed in a stepwise sequential process, starting with cut-off grade optimization through Lane's method, defining the cut-off grade policy over the life of the mine. Next, production scheduling is conducted, defining when and where material is to be extracted from the pit. Lastly, down stream decisions are determined, defining where and how material should be treated. However, all of these components are interdependent, meaning that the sequential process provides a locally optimal mine plan, rather than a globally optimal mine plan. Additionally, traditional mine planning is deterministic, ignoring the uncertainty inherent in mine planning. Recent stochastic methods have improved upon the traditional framework by considering uncertainty, and simultaneously optimizing all components of the mineral value chain under one mathematical formulation. However, both the traditional and state of the art stochastic approaches do not (1) consider equipment access when optimizing production schedules, and (2) provide optimal multi-element cut-off grades under supply uncertainty. These observations motivated the development of two stochastic methods to address the noted limitations, while considering geological uncertainty. The first method presented in this thesis jointly optimizes production schedules and ramp design, while ensuring feasible equipment access to mined blocks. The second method determines optimal multi-element cut-off policy over the life-of-mine for an optimal production plan.

The first method presented in Chapter 2 jointly optimizes long-term open pit mine production schedules and ramp design while ensuring equipment access to mined blocks under geological uncertainty. The proposed two-stage SIP maximizes NPV, while considering the cost of constructing and removing ramps and managing deviations from targets. The method outputs a long-term production schedule and ramp design, defining when, where ramps should be placed and what designs ramps should have. The method guarantees that some road surface exists from all mined blocks to the surface of the pit, where the road surface may only change benches through ramps, ensuring that equipment can access all scheduled blocks. The method is applied to a gold mine, and the optimized production schedule and ramp design are presented. Each ramp segment is placed tightly against the left side of the pit wall, minimizing the quantity of trapped ore beneath the ramp. Though ramps could have been removed or added, the optimizer only placed the minimal number of ramps required to reach the bottom of the pit, and never modified a ramp segment after placement. The schedule focused most mining activity on the left pit walls in the early years to (1) provide space to place ramp segments and (2) provide early access to ore, enabling the production schedule to meet production forecasts.

The second method, presented in Chapter 3 determines the optimal multi-element cut-off grade policy over the life-of-mine for an optimal production plan under geological uncertainty. A reinforcement learning framework is presented, leveraging PPO to minimize deviations between optimal production forecasts, and multi-element cut-off grade forecasts. The method is applied to a gold-copper mining complex that was optimized using the state-of-the-art simultaneous stochastic optimization of mining complexes framework, and two multi-element cut-off grades were tested, orthogonal and diagonal. The cut-off grades were optimized to minimize deviations from optimal mill metal production, mill tonnage, and stockpile tonnage. Both multi-element cut-off grades were found to perform well, largely reproducing the optimal production forecasts. However, the diagonal policy was found to perform slightly better.

4.1 Recommendations for Future Research

Future research on the proposed topics can build upon both methods in numerous ways. Integrating the join stochastic optimization of long-term open pit mine production schedules into the simultaneous stochastic optimization of mining complexes framework would provide significant value as equipment access constraints drive large changes in the production schedule. Simultaneously considering the impacts of such changes on the destination policy, and downstream decisions may contribute to significantly altered mine plans and forecasts. Additionally, the method could be extended to consider the cost of roads, and optimize their design, rather than simply ensuring a possible road surface exists. The second method could benefit from further investigation into alternative cut-off grade designs, and more testing on larger mining complexes with more destinations and elements.

Chapter 5. References

Abramowitz M, and Stegun I A (1964). Handbook of Mathematical Functions with Formulas, Graphs, and Mathematical Tables. Dover, New York.

Asad M W A (2005). Cutoff grade optimization algorithm with stockpiling option for open pit mining operations of two economic minerals. International Journal of Surface Mining, Reclamation and Environment 19(3): 176-187.

Asad M W A, and Dimitrakopoulos R (2013). A heuristic approach to stochastic cutoff grade optimization for open pit mining complexes with multiple processing streams. Resources Policy 38(4): 591-597.

Asad M W A, Qureshi M A, and Jang H (2016). A review of cut-off grade policy models for open pit mining operations. Resources Policy 49: 142-152.

Baker C K, and Giacomo S M (2001). Resources and reserves: Their uses and abuses by the equity markets. 23: 667-676.

Benndorf J, and Dimitrakopoulos R (2013). Stochastic long-term production scheduling of iron ore deposits: Integrating joint multi-element geological uncertainty. Journal of Mining Science 49(1): 68-81.

Birge R J, and Louveaux F (2011). Introduction to Stochastic Programming. Springer, New York, NY.

Boland N, Dumitrescu I, and Froyland G (2008). A multistage stochastic programming approach to open pit mine production scheduling with uncertain geology.

Boucher A, and Dimitrakopoulos R (2007). A new efficient joint simulation framework and application in a multivariable deposit. Orebody modelling and strategic mine planning. Spectrum series 14: 345-354.

Boucher A, and Dimitrakopoulos R (2009). Block Simulation of Multiple Correlated Variables. Mathematical Geosciences 41(2): 215-237.

David M (1977). Geostatistical Ore Reserve Estimation. Elsevier Science.

David M (1988). Handbook of applied advanced geostatistical ore reserve estimation. Elsevier : Distributors for the United States and Canada Elsevier Science Pub. Co., Amsterdam, New York.

Davis M W (1987). Production of Conditional SImulations via the LU Triangular Decomposition of the Covariance Matrix. Mathematical Geology.

de Carvalho J P, and Dimitrakopoulos R (2019). Effects of High-Order Simulations on the Simultaneous Stochastic Optimization of Mining Complexes. Minerals 9(4): 210.

De Carvalho J P, Dimitrakopoulos R, and Minniakhmetov I (2019). High-Order Block Support Spatial Simulation Method and Its Application at a Gold Deposit. Mathematical Geosciences 51(6): 793-810.

Del Castillo M F, and Dimitrakopoulos R (2019). Dynamically optimizing the strategic plan of mining complexes under supply uncertainty. Resources Policy 60: 83-93.

Desbarats A J, and Dimitrakopoulos R (2000). Geostatistical SImulation of Regionalized Pore-Size Distributions Using Min/Max Autocorrelation Factors. Mathematical Geology 32(8): 919-942.

Dimitrakopoulos R, Farrelly C T, and Godoy M (2002). Moving forward from traditional optimization: grade uncertainty and risk effects in open-pit design. Mining Technology 111(1): 82-88.

Dimitrakopoulos R, and Jewbali A (2013). Joint stochastic optimisation of short and long term mine production planning: method and application in a large operating gold mine. Mining Technology 122(2): 110-123.

Dimitrakopoulos R, and Lamghari A (2022). Simultaneous stochastic optimization of mining complexes - mineral value chains: an overview of concepts, examples and comparisons. International Journal of Mining, Reclamation and Environment 36(6): 443-460.

Dimitrakopoulos R, and Luo X (2004). Generalized Sequential Gaussian Simulation on Group Size and Screen-Effect Approximations for Large Field Simulations. Mathematical Geology 36(5): 567-591.

Dimitrakopoulos R, Martinez L, and Ramazan S (2007). A maximum upside / minimum downside approach to the traditional optimization of open pit mine design. Journal of Mining Science 43(1): 73-82.

Dimitrakopoulos R, Mustapha H, and Gloaguen E (2010). High-order Statistics of Spatial Random Fields: Exploring Spatial Cumulants for Modeling Complex Non-Gaussian and Non-linear Phenomena. Mathematical Geosciences 42(1): 65-99.

Dimitrakopoulos R, and Ramazan S (2008). Stochastic integer programming for optimising long term production schedules of open pit mines: methods, application and value of stochastic solutions. Mining Technology 117(4): 155-160.

Dowd P (1994). Risk assessment in reserve estimation and open-pit planning. Transactions of the Institution of Mining and Metallurgy, Section A: Mining Technology 103: 148-154.

Dowd P (1997). Risk in minerals projects: analysis, perception and management. TRANSACTIONS OF THE INSTITUTIONS OF MINING AND METALLURGY SECTION A-MINING TECHNOLOGY 106: A9-A18.

Farmer I (2016). Stochastic Mining Supply Chain Optimization: A Study of Integrated Capacity Decisions and Pushback Design Under Uncertainty. Mining and Materials Engineering. Montreal, McGill University Mining Engineering 97.

Fix E, and Hodges J L (1989). discriminatory analysis nonparametric discrimination: consistency properties. International Statistical Review / Revue Internationale de Statistique 57(3): 238.

Ganguli R, Dagdelen,K.,Grygiel,E. (2011). Minescheduling andc ut-off grade optimization using mixed integer linear programming. SME Mining Engineering Handbook

Gill T (1999). Express Road Routing: The Application of an Optimal Haul Road Generator to Real World Data. Optimizing with Whittle. Perth, Whittle: 411-422.

Godoy M (2004). Managing Risk and Waste Mining in Long-Term Production Planning of Open Pit Mine. SME Ann Meet Exhib 316: 43-50.

Godoy M C (2003). The effective management of geological risk in long-term production scheduling of open pit mines. School of Engineering, The University of Queensland. PsD: 256.

Goodfellow R (2014). Unified Modelling and Simultaneous Optimization of Open Pit Mining Complexes with Supply Uncertainty. Mining and Materials Engineering. Montreal, Quebec, McGill University. Doctor of Philosophy: 274.

Goodfellow R, Albor Consuegra F, Dimitrakopoulos R, and Lloyd T (2012). Quantifying multi-element and volumetric uncertainty, Coleman McCreedy deposit, Ontario, Canada. Computers & Geosciences 42: 71-78.

Goodfellow R, and Dimitrakopoulos R (2016). Global optimization of open pit mining complexes with uncertainty. Applied Soft Computing 40: 292-304.

Goodfellow R, and Dimitrakopoulos R (2017). Simultaneous Stochastic Optimization of Mining Complexes and Mineral Value Chains. Mathematical Geosciences 49(3): 341-360.

Goodfellow R C, and Dimitrakopoulos R (2016). Global optimization of open pit mining complexes with uncertainty. Applied Soft Computing Journal 40: 292-304.

Goovaerts P (1997). Geostatistics for Natural Resource Evaluation. Oxford University Press, New York, NY.

Gravey M, and Mariethoz G (2020). QuickSampling v1.0: a robust and simplified pixel-based multiple-point simulation approach. Geoscientific Model Development 13(6): 2611-2630.

Guardiano F B, and Srivastava R M (1993). Multivariate Geostatistics: Beyond Bivariate Moments. Quantitative Geology and Geostatistics, Springer Netherlands: 133-144.

Hansen P, and Mladenović N (2001). Variable neighborhood search: Principles and applications. European Journal of Operational Research 130(3): 449-467.

Hochbaum D (2008). The Pseudoflow Algorithm: A New Algorithm for the Maximum-Flow Problem. Operations Research 56: 992-1009.

Hoerger S, Hoffman L, and Seymour F (1999). Mine planning at Newmont's Nevada operations. Mining Engineering 51(10): 26.

Howard R A (1960). Dynamic programming and Markov processes. John Wiley, Oxford, England.

Hustrulid W A, Kuchta M, and Martin R K (2013). Open Pit Mine Planning and Design. CRC Press, Boca Raton, FL.

Isaaks E H, and Srivastava R M (1989). Applied Geostatistics. Oxford University Press.

Journel A G (2003). Multiple-point Geostatistics : A State of the Art.

Journel A G, and Deutsch C V (1993). Entropy and spatial disorder. Mathematical Geology 25(3): 329-355.

Journel A G, and Huijbregts C J (1978). Mining Geostatistics. Academic Press.

Khan A, and Asad M W A (2019). A method for optimal cut-off grade policy in open pit mining operations under uncertain supply. Resources Policy 60: 178-184.

Kirkpatrick S, Gelatt C D, and Vecchi M P (1983). Optimization by Simulated Annealing. Science 220(4598): 671-680.

Knuth D E (1997). The Art of Computer Programming. Addison-Wesley, Boston, MA.

Kumar A, and Dimitrakopoulos R (2019). Application of simultaneous stochastic optimization with geometallurgical decisions at a copper–gold mining complex. Mining Technology 128(2): 88-105.

Lamghari A, and Dimitrakopoulos R (2012). A diversified Tabu search approach for the open-pit mine production scheduling problem with metal uncertainty. European Journal of Operational Research 222(3): 642-652.

Lamghari A, and Dimitrakopoulos R (2020). Hyper-heuristic approaches for strategic mine planning under uncertainty. Computers & Operations Research 115: 104590.

Lamghari A, and Dimitrakopoulos R (2022). An adaptive large neighborhood search heuristic to optimize mineral value chains under metal and material type uncertainty. International Journal of Mining, Reclamation and Environment 36(1): 1-25.

Lamghari A, Dimitrakopoulos R, and Ferland J A (2014). A variable neighbourhood descent algorithm for the open-pit mine production scheduling problem with metal uncertainty. Journal of the Operational Research Society 65(9): 1305-1314.

Lane K F (1964). Choosing the optimum cut-off grade. Colorado School of Mines Quarterly 59: 11-29.

Lane K F (1988). The Economic Definition of Ore: Cut-off Grades in Theory and Practice. Mining Journal Books.

Leite A, and Dimitrakopoulos R (2007). Stochastic optimisation model for open pit mine planning: application and risk analysis at copper deposit. Mining Technology 116(3): 109-118.

Lerchs H, and Grossman I F (1965). Optimum Design of Open Pit Mines. CIM 68: 17-24.

Macneil J A L, and Dimitrakopoulos R G (2017). A stochastic optimization formulation for the transition from open pit to underground mining. Optimization and Engineering 18(3): 793-813.

Mariethoz G, Renard P, and Straubhaar J (2010). The Direct Sampling method to perform multiple-point geostatistical simulations. Water Resources Research 46(11).

Menabde M, Froyland G, Stone P, and Yeates G A (2018). Mining Schedule Optimisation for Conditionally Simulated Orebodies. Advances in Applied Strategic Mine Planning, Springer International Publishing: 91-100.

Minniakhmetov I, and Dimitrakopoulos R (2017). Joint High-Order Simulation of Spatially Correlated Variables Using High-Order Spatial Statistics. Mathematical Geosciences 49(1): 39-66.

Minniakhmetov I, and Dimitrakopoulos R (2022). High-Order Data-Driven Spatial Simulation of Categorical Variables. Mathematical Geosciences 54(1): 23-45.

Minniakhmetov I, Dimitrakopoulos R, and Godoy M (2018). High-Order Spatial Simulation Using Legendre-Like Orthogonal Splines. Mathematical Geosciences 50(7): 753-780.

Montiel L, and Dimitrakopoulos R (2013). Stochastic mine production scheduling with multiple processes: Application at Escondida Norte, Chile. Journal of Mining Science 49(4): 583-597.

Montiel L, and Dimitrakopoulos R (2015). Optimizing mining complexes with multiple processing and transportation alternatives: An uncertainty-based approach. European Journal of Operational Research 247(1): 166-178.

Montiel L, and Dimitrakopoulos R (2017). A heuristic approach for the stochastic optimization of mine production schedules. Journal of Heuristics 23(5): 397-415.

Montiel L, and Dimitrakopoulos R (2018). Simultaneous stochastic optimization of production scheduling at Twin Creeks Mining Complex, Nevada. Mining Engineering 70(12): 48-56.

Montiel L, Dimitrakopoulos R, and Kawahata K (2016). Globally optimising open-pit and underground mining operations under geological uncertainty. Mining Technology 125(1): 2-14.

Morales N, Nancel-Penard P, and Espejo N (2023). Development and analysis of a methodology to generate operational open-pit mine ramp designs automatically. Optimization and Engineering 24(2): 711-741.

Mustapha H, and Dimitrakopoulos R (2010). High-order Stochastic Simulation of Complex Spatially Distributed Natural Phenomena. Mathematical Geosciences 42(5): 457-485.

Mustapha H, and Dimitrakopoulos R (2010). A new approach for geological pattern recognition using high-order spatial cumulants. Computers & Geosciences 36(3): 313-334.

Nancel-Penard P, Parra A, Morales N, Díaz C, and Widzyk-Capehart E (2019). Value-optimal design of ramps in open pit mining. Archives of Mining Sciences 64(2): 399-413.

Osterholt V (2007). Resource model uncertainty at the yandi channel iron deposits, western Australia - An application of multiple-point simulation for orebody geology. Australasian Institute of Mining and Metallurgy Publication Series: 147-151.

Pimentel B, Mateus G, and Assunção Almeida F (2010). Mathematical Models for Optimizing the Global Mining Supply Chain. Intelligent Systems in Operations: Methods, Models and Applications in the Supply Chain: 133-163.

Quigley M, Dimitrakopoulos R, and Grammatikopoulos T (2018). Risk-resilient mine production schedules with favourable product quality for rare earth element projects. Mining Technology 127(1): 41-55.

Ramazan S (2004). Uncertainty-based production scheduling in open pit mining. Transactions, Society of Mining, Metalurgy and Exploration 316: 106-112.

Ramazan S, and Dimitrakopoulos R (2005). Stochastic Optimization Of Long-term Production Scheduling For Open Pit Mines With A New Integer Programming Formulation. Orebody modelling and strategic mine planning, Springer, Cham: 353-360.

Ramazan S, and Dimitrakopoulos R (2013). Production scheduling with uncertain supply: a new solution to the open pit mining problem. Optimization and Engineering 14(2): 361-380.

Ravenscroft P (1992). Risk analysis for mine scheduling by conditional simulation. Transactions of the Institution of Mining and Metallurgy. Section A. Mining Industry 101.

Rendu J M (2014). An introduction to cut-off grade estimation, second edition. Society for Mining, Metallurgy & Exploration, Incorporated, Inglewood, CO.

Rossi M E, and Deutsch C V (2014). Mineral resource estimation. Dordrecht, Springer.

Schulman J, Wolski F, Dhariwal P, Radford A, and Klimov O (2017). proximal policy optimization algorithms. ArXiv abs/1707.06347.

Seymour F (1995). Pit Limit Parameterization From Modified 3D Lerchs-Grossmann Algorithm. Society for Mining, Metallurgy, and Exploration, INC.

Stone P, Froyland G, Menabde M, Law B, Rasyar R, and Monkhouse P (2004). Blasor – Blended iron-ore mine planning optimisation at Yandi". Orebody Modelling and Strategic Mine Planning. Proceedings of the International Symposium: 285-288.

Straubhaar J, Renard P, Mariethoz G, Froidevaux R, and Besson O (2011). An Improved Parallel Multiple-point Algorithm Using a List Approach. Mathematical Geosciences 43(3): 305-328.

Strebelle S (2002). Conditional Simulation of Complex Geological Structures Using Multiple-Point Statistics. Mathematical Geology 34(1): 1-21.

Sutton R S, and Barto A G (2018). Reinforcement learning: An introduction, 2nd ed. The MIT Press, Cambridge, MA, US.

Vallee M (2000). Mineral resource + engineering, economic and legal feasibility = ore reserve. CIM BULLETIN(1038): 53-61.

Vargas-Guzmán J A, and Dimitrakopoulos R (2002). Conditional Simulation of Random Fields by Successive Residuals. Mathematical Geology 34(5): 597-611.

Whittle J (2007). Global asset optimisation. Orebody modelling and strategic mine planning. Spectrum series.

Whittle J (2018). The Global Optimiser Works—What Next? Advances in Applied Strategic Mine Planning, Springer International Publishing: 31-37.

Wu J, Zhang T, and Journel A (2008). Fast FILTERSIM Simulation with Score-based Distance. Mathematical Geosciences 40(7): 773-788.

Yaakoubi Y, and Dimitrakopoulos R (2023). Learning to schedule heuristics for the simultaneous stochastic optimization of mining complexes. Computers & Operations Research 159: 106349.

Yao L, Dimitrakopoulos R, and Gamache M (2018). A New Computational Model of High-Order Stochastic Simulation Based on Spatial Legendre Moments. Mathematical Geosciences 50(8): 929-960.

Yao L, Dimitrakopoulos R, and Gamache M (2021). Training Image Free High-Order Stochastic Simulation Based on Aggregated Kernel Statistics. Mathematical Geosciences 53(7): 1469-1489.

Yarmuch J, Brazil M, Rubinstein H, and Thomas D (2020). Optimum ramp design in open pit mines. Computers & Operations Research 115: 104739.

Yarmuch J L, Brazil M, Rubinstein H, and Thomas D A (2021). A mathematical model for mineable pushback designs. International Journal of Mining, Reclamation and Environment 35(7): 523-539.

Zhang J, and Dimitrakopoulos R G (2017). A dynamic-material-value-based decomposition method for optimizing a mineral value chain with uncertainty. European Journal of Operational Research 258(2): 617-625.

Zhang T, Switzer P, and Journel A (2006). Filter-Based Classification of Training Image Patterns for Spatial Simulation. Mathematical Geology 38(1): 63-80.